Design and Prototype of an Active Knee Exoskeleton to Aid Farmers with Mobility Limitations

Evan A. Wood

Thesis submitted to the Faculty of the
Virginia Polytechnic Institute and State University
in partial fulfillment of the requirements for the degree of

Master of Science
in
Mechanical Engineering

Alan T. Asbeck, Chair
Alexander Leonessa
Divya Srinivasan

August 8, 2019
Blacksburg, Virginia

Keywords: Active Exoskeleton, capability augmentation, Knee joint

Design and Prototype of an Active Knee Exoskeleton to Aid Farmers with Mobility Limitations

Evan A. Wood

(ABSTRACT)

This paper presents an active knee exoskeleton determined to aid an increasingly aging farmers population with mobility limitations due to factors such as disease, age and prior injuries. The exoskeleton utilizes a system of distally worn quadcopter motors, Bowden cable and pulleys to provide assistive torque to the wearer at the knee joint. An assistive torque of 30% of the required knee torque to perform daily activities (e.g., sit to stand, ascension/descension of stairs and hills) is intended to be produced by the exoskeleton aiming to reduce stress on the wearer's knees, increase range of motion and decrease possibility of secondary injuries. The mechatronic design and control scheme of the exoskeleton is further described.

Design and Prototype of an Active Knee Exoskeleton to Aid Farmers with Mobility Limitations

Evan A. Wood

(GENERAL AUDIENCE ABSTRACT)

As farmers continue to get older, they will likely face age-related disabilities that impede their ability to work and increase risk of suffering serious injuries. One of the major age-related diseases is arthritis, which currently accounts for about 40% of disability cases in agriculture nationwide. The effect of arthritis on farmers is profound because it reduces their physical strength, joint range of motion and is a source of joint pain, all culminating in the lack of ability to perform routine activities regularly and safely. One way to decrease the rate of injuries is by reducing the strength and joint loading required to perform these activities through the use of wearable robotics. As opposed to existing solutions that focus only on injury prevention, this thesis will present an active, knee-assist exoskeleton intent on providing 30% of the necessary joint rotation force to perform activities such as sit-to-stand actions and the ascent/descent of stairs and hills. The device will be a lightweight, unobtrusive cable-driven exoskeleton actuated by distally-worn electric motors. We hope that use of the exoskeleton will result in increased ranges of motion and overall reduction of stress on the wearer's body, which will minimize the effects of arthritis and ultimately improve safety and quality of life.

Acknowledgments

I would like to thank my committee chairman Dr. Alan Asbeck for granting me the opportunity to join the Assistive Robotics Lab. Under Dr. Asbeck's guidance I have been exposed to so many different aspects of engineering and as a result have developed a well rounded skill set that will help me in my future as an engineer. I would also like to thank Dr. Queen and Dr. Leonessa for serving on my advisory committee.

Thank you to my lab mates, Tim, Athulya, Hee Doo, Caleb, Hani and Jack that helped, provided input and supported me and my project. I would like to give a special thanks to Brandyn Greczek for his valuable input and assistance in several aspects of the development of this exoskeleton. I would also like to thank Hubert Kim for his assistance and guidance in programming and debugging. Thank you to Taylor Pesek for his valuable assistance, advice and efforts to help me with prototyping issues. Thank you to the undergraduate students, Andrew, Evan and Tom that assisted in the assembly of an exoskeleton prototype.

Finally, I would like to thank my family and friends for their endless support throughout my pursuit of a Masters degree. Your encouragement, advice and motivation meant the world to me.

Contents

List of Figures

List of Tables

List of Abbreviations

η	efficiency
ω_m	angular velocity
τ	Torque
I_a	Current Applied
k_e	Speed Constant
k_t	Torque Constant
P_m	Mechancial Power
R_a	Resistance
AAN	Assistance As Needed
ADL	Activities of daily living
BLDC	Brushless Direct Current
EMG	Electromyography
FBD	Free Body Diagram
FEA	finite element analysis
IMU	Inertial Measurement Unit
kg	kilogram

MCU Microcontroller Unit

N Gear-reduction

N Newton

Nm Newton-meter

PD Proportional-Derivative

PWM Pulse Width Modulation

ROM Range of Motion

rpm revolutions per minute

SEA Series Elastic Actuator

STS Sit to Stand

USDA United States Department of Agriculture

V Voltage

Attribution

I contributed extensively to the ideation, design and build of the exoskeleton presented in this thesis. I have contributed from the initial phases of conception to its current state. In the conception phase I was fully responsible for conducting biomechanical and exoskeleton literature review to establish initial project goals and requirements based on human motion requirements. I digitized angle, torque and velocity values from biomechanical literature to be used in the application and design of a control structure. I was also vital in the decision to use a distally placed actuator and Bowden cable driven system. After ideation, I was responsible for the design, CAD modeling and finite element analysis of the entire exoskeleton system. I also was in charge of motor-gearbox selection and analysis to satisfy biomechanical joint torque and speed requirements, actuator design, sensor and microcontroller selection and integration, and printed circuit board design for instrumentation breakout.

In addition to design responsibilities, I performed manufacturing, wiring and assembly of an exoskeleton prototype and was responsible for the programming of a control system that allows the exoskeleton to perform an angle based torque application. I also wrote code for data logging using serial communication and Matlab script to post-process and graph collected data for easier analysis. My final contribution is this thesis, documenting all design choices and construction of this active knee exoskeleton.

Chapter 1

Introduction

In recent years, a great deal of research has been dedicated to the development of solutions aimed at enabling people who are unable to easily perform activities of daily living (ADL) due to age, injury or disease. One solution researchers continue to explore are wearable robotics known as exoskeletons, they can either augment or rehabilitate a wearer's strength and endurance through passive or active assistance. Passive exoskeletons avoid the use of motors or batteries and provide assistance through mechanical means such as springs, material properties, dampers or locking mechanisms [19,20]. A passive system will store energy harvested by human motion and use it to support posture or motion [21] but they typically lack the ability to provide the level of assistance possible with active exoskeletons. Active exoskeletons use a variety of powered actuation methods such as cable driven, hydraulic, pneumatic, direct drive electric or series elastic actuators (SEA) to create large assistance forces capable of bridging the gap between a wearer's ability and task requirements.

The exoskeleton presented in this work is a cable driven, active knee exoskeleton designed to assist an aging population of farmers perform the activities of sit to stand (STS) and hill and stair navigation. While performing these everyday activities, older farmers tend to struggle due to loss of muscle, age-related disease or decreased range of motion (ROM) and it can cause over-straining of muscles and joints or improper technique which can result in serious injury and greatly increased energy expenditure. Through the use of a distally placed brushless motor and Bowden cable for force transmission, the exoskeleton is able to

generate a torque at the knee capable of assisting the wearer throughout their motion, thus improving their ability to perform ADL and relieving the strain on their joints. The design and development of the exoskeleton are further discussed.

1.1 Background and Motivation

Agriculture plays a significant role in the lives of all members of the population through the production of food and raw materials that form the basis of society. At the heart of such an industry is an aging population of farmers working hard to maintain and provide for society. Sometimes these farmers struggle to perform the activities required to successfully farm and reach their daily goals often due to age related disabilities or injuries that impede their ability to work. According to the United States Department of Agriculture (USDA) the age of farmers is currently at a national average of 58.3 years old and about one-third of established farmers are over 65 [1]. Moreover, consistent with a thirty year trend the average age continues to increase, with a 2.1% increase coming between 2007 and 2012. Figure 1.1 depicts the 2014 USDA's report on the past and present average age of farmers.

An increasingly older farmer population presents challenges to both society and the individual farmer. As age climbs, the issue of disabilities such as arthritis, limited mobility and less tolerability to body stresses become more prevalent, often resulting in injuries that impede their ability to perform ADL, decrease productivity and further increase the risk of suffering a more serious or even fatal injury. Arthritis is one of the most common diseases, affecting 1 in 5 Americans and accounts for about 30% of the disability cases in agriculture [22]. The effect of arthritis is profound because it severely reduces strength, range of motion (ROM), has a negative effect on quality of life and is often a reason for injury. Several studies have been conducted to examine the relationship between arthritis and farm related injuries

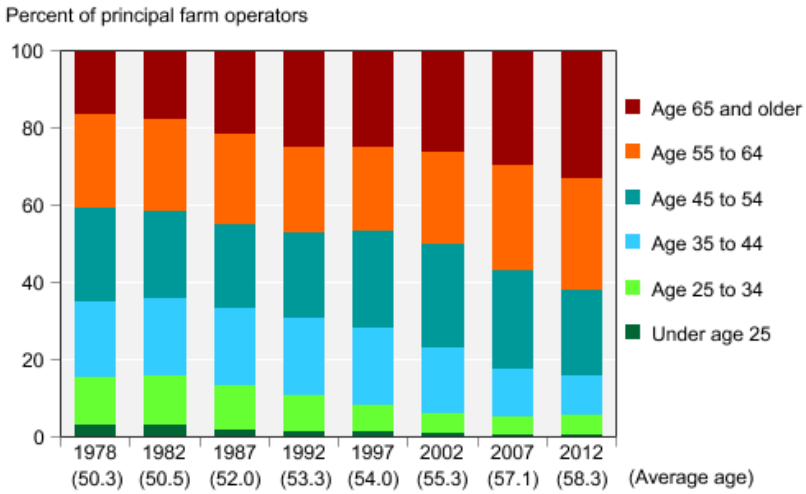

Figure 1.1: 2014 USDA census of average age of farmers[1]

[23,24,25] with some finding that an injury occurring with arthritis is 2.6 times more likely than without [24].

During a farmer's day they are required to perform activities such as tending to crops or animals, climbing in and out of machinery and lifting heavy objects. Movements essential to performing those duties include STS and the ability to ascend and descend stairs or hills; which often present extreme challenges to those with muscle weakness and limited ROM because they involve a phase of instability, maximum moments in the lower body joints and require a greater amount of force than normal walking. For example, during stair or hill descent forces at the knee can be 2-3x the force required of level ground walking. STS causes issue as rising from a chair requires a transfer of mass from seated to standing position resulting in a peak moment on the knee joint in conjunction with a moment of instability [26].

One approach to assisting aging farmers, decreasing the risk of injury and overall improving the quality of life is by deloading joints that have the greatest negative impact on farmers with disabilities, such as the knee. One of the most promising technological developments

to accomplish such a task are exoskeletons. Exoskeletons are devices designed to work in conjunction with the wearer to provide part or the entire force required to perform specific activities. Depending on the method for providing assistive forces the exoskeleton can be passive or active. Current exoskeletons are versatile and have been developed for military, industrial and rehabilitation applications [27]. Some of the most promising industrial and rehabilitation exoskeletons include Ekso Bionic's EksoGT, Cyberdine HAL 5 exoskeleton and Laevo.

1.2 Research Goals

This thesis is part of a National Science Foundation: partnership for innovation project to develop flexible robotic systems that are wearable by farmers with mobility limitations to assist them with ADL. The goal of this thesis is to design and develop an active knee exoskeleton that can bridge the gap between the capabilities of the wearer and the force required to perform everyday movements.

The following are specific goals of this thesis:

- Determine the knee joint angle, speed and torque required to perform STS and stair/hill climbing and descent
- Apply human biomechanical data to establish requirements for the design of an exoskeleton capable of assisting farmers in their ADL
- Design and analysis of an exoskeleton capable of providing up to 30% of the necessary knee torque for sit to stand, stair and hill negotiation
- Evaluation of the manufactured knee exoskeleton and a discussion of its performance

1.3 Thesis Organization

The design and development of an active knee exoskeleton are discussed in this thesis. In the following section we examine the biomechanical requirements of performing STS and stair/hill ascent and descent, then review the prior research conducted on active exoskeletons. The joint torque, speed and wearability design requirements are discussed in chapter 3. Chapter 4 contains detail explanation of the design and analysis of the components that constitute the exoskeleton. Performance evaluation of the manufactured exoskeleton are presented in chapter 5. Chapter 6 provides conclusion to this research and presents possible future work for this project.

Chapter 2

Literature Review

This chapter is divided into two sections. The first section focuses on the research that has been conducted on the biomechanical parameters of the knee during STS and stair/hill ascent and descent activities. The second section presents the literature on a few examples of prior developed active exoskeletons and their applications.

2.1 Biomechanical Background

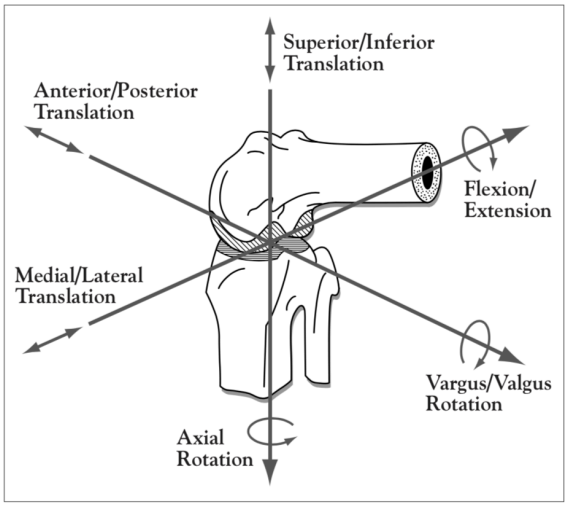

Figure 2.1: 6 Degrees of Freedom within the Knee Joint, characterized as 3 translational and 3 rotational motions [2]

Many studies have been conducted to better understand knee anatomy and biomechanics. The knee joint is relatively complex, possessing six degrees of freedom including three ro-

tations, flexion/extension, internal/external rotation and varus/valgus angulation and three translations, anterior/posterior glide, medial/lateral shift and compression/distraction (Figure 2.1) [2]. It operates through a combination of rolling and sliding between the femur and tibia, allowing the center of rotation to move as the knee flexes [28].

The following will present prior work of studies performed to understand knee biomechanics, focusing on the knee moment, angle, and velocity data collected through prior research. Through understanding this data we will be able to establish the design requirements of an active assistive knee exoskeleton.

2.1.1 Sit To Stand

STS movement is an important action performed by farmers in a variety of ways ranging from rising from a knee when inspecting crops, getting out of machinery or just standing up from the kitchen table. STS has been the focus of several studies in an effort to understand the different factors affecting STS movement, phases of motion and ultimately the biomechanical requirements of performing STS [3,26,29,30,31,].

In conducting a STS study, researchers must understand the different factors of movement. These factors are divided into three groups: subject related, strategy related and chair related [32]. Subject related includes disease or injury history, age, and weight. A few studies have been conducted to attempt to quantify the effects of these factors on biomechanical parameters involved in STS [29,30]. Strategy related factors include parameters that can be defined within the experimental methods, for example foot position, trunk movement, arm position, speed of STS movement, and training. The third group of factors are chair related and cover height of chair, chair with armrests, and special types of chairs[32].

There are two popular definitions for dividing the STS movement into phases. The first

defines STS into three phases: acceleration phase, transition phase and deceleration phase [3]. The acceleration phase represents the period in which the center of mass is accelerated horizontally and typically lasts from the beginning of movement to maximum horizontal velocity. The transition phase happens when the center of mass begins decelerating horizontally and accelerating vertically, ending at maximal vertical velocity. During this phase seat-off occurs at 35% of total movement time. In the last phase, deceleration occurs from maximal vertical velocity to end of movement [3]. Figure 2.2 shows a three phase velocity graph for both horizontal and vertical velocities.

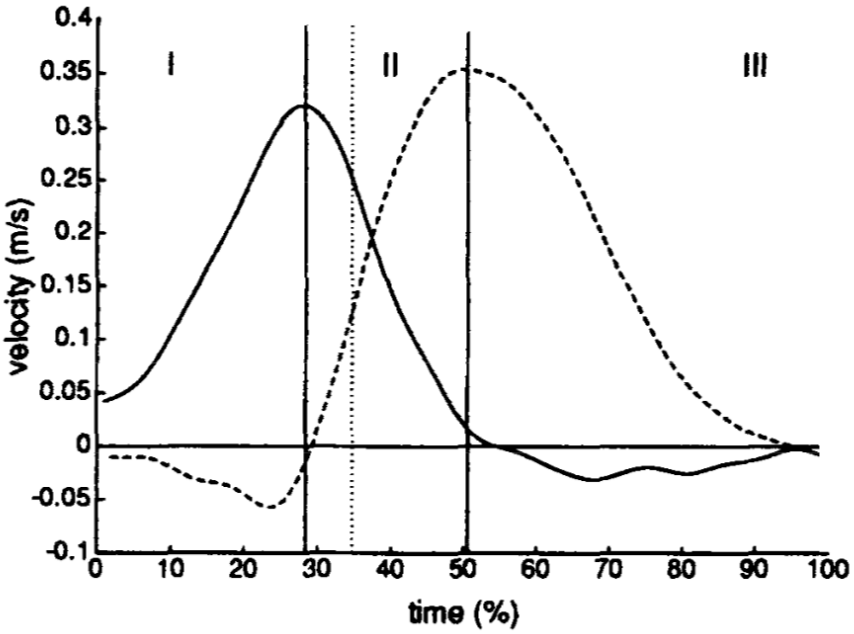

Figure 2.2: Horizontal and Vertical velocities of STS motion divied into three phases. (solid line = horizontal, dashed = vertical)[3]

The second definition separates STS movement into four phases. The first phase is flexion momentum in which movement is initiated, the upper body is rotated anteriorly to generate momentum and ends at the beginning of seat off. The next phase, momentum-transfer begins with seat off and ends with maximum ankle dorsiflexion. During this phase, momentum from the trunk is transferred to total body and contributes to upward movement. The third phase

is extension and is defined to occur from maximum ankle dorsiflexion to the time at which hip extension velocity has reached a velocity of 0° per second. Maximum hip, trunk and knee extension velocities are met during the third phase. In the fourth phase, stabilization occurs from the maximum vertical velocity to the end of movement. The four phases are shown in figure 2.3.

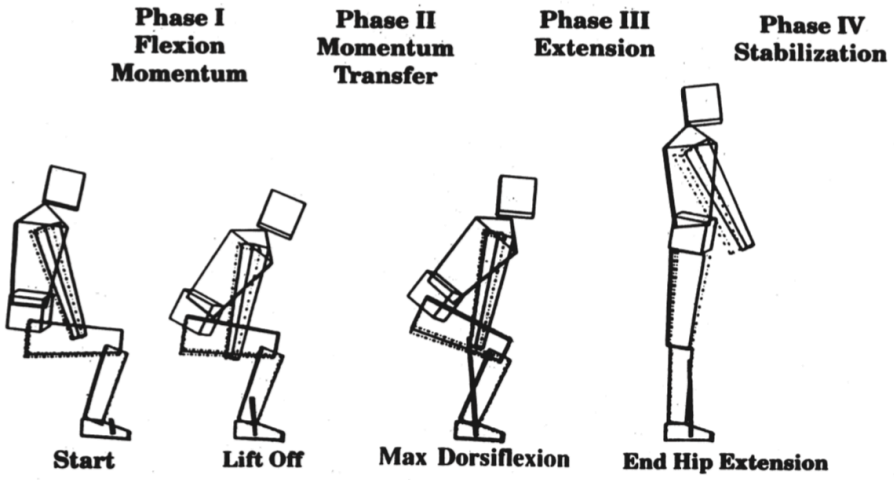

Figure 2.3: Four phase STS movement[4]

Various studies have been conducted to gather the moment, angle, velocity and acceleration data of the knee to successfully complete STS movement. Table 2.1 presents some of the knee moments collected from literature. It can be noted from Table 2.1 that the data for knee moments vary due to factors such as experimental methods, study participants and a lack of complete understanding of human motion contributing to differences in results. Moreover, it has been observed that elderly individuals perform STS differently than healthy young adults by using more trunk flexion, thus increasing hip flexion and decreasing knee extension[30]. Knee angle and velocity are presented in figure 2.4 and 2.5 respectively.

Author	Knee Moment(Nm/kg)
Roebreck, 1994 [3]	0.88
Yoshioka, 2014 [31]	0.75
Sibella, 2003 [29]	0.45
Gross, 1998 [33]	1.51

Table 2.1: Knee Moment Data from Literature

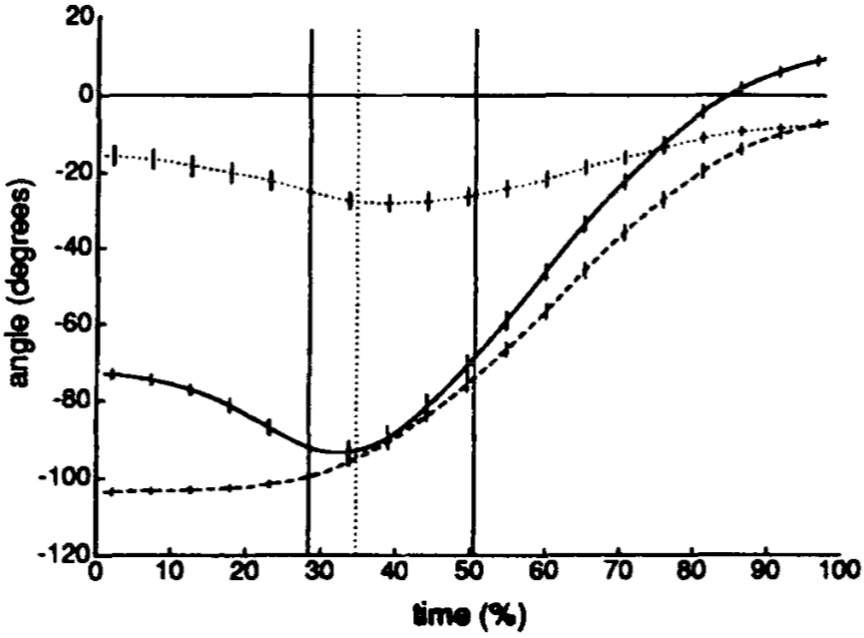

Figure 2.4: Joint angles during STS for hip (solid), Knee(dashed) and ankle(dotted line) [3]

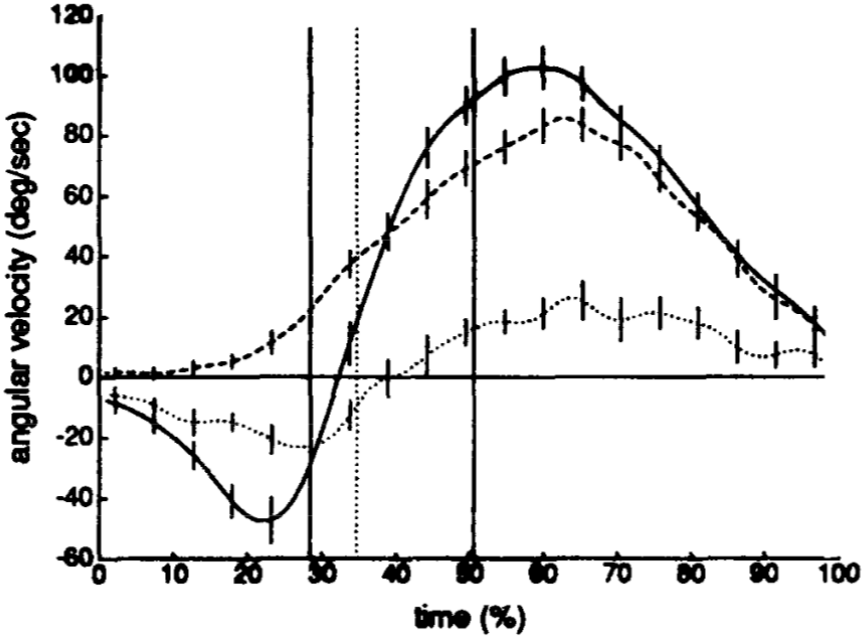

Figure 2.5: Joint velocities during STS for hip (solid line), knee (dashed) and ankle (dotted line)[3]

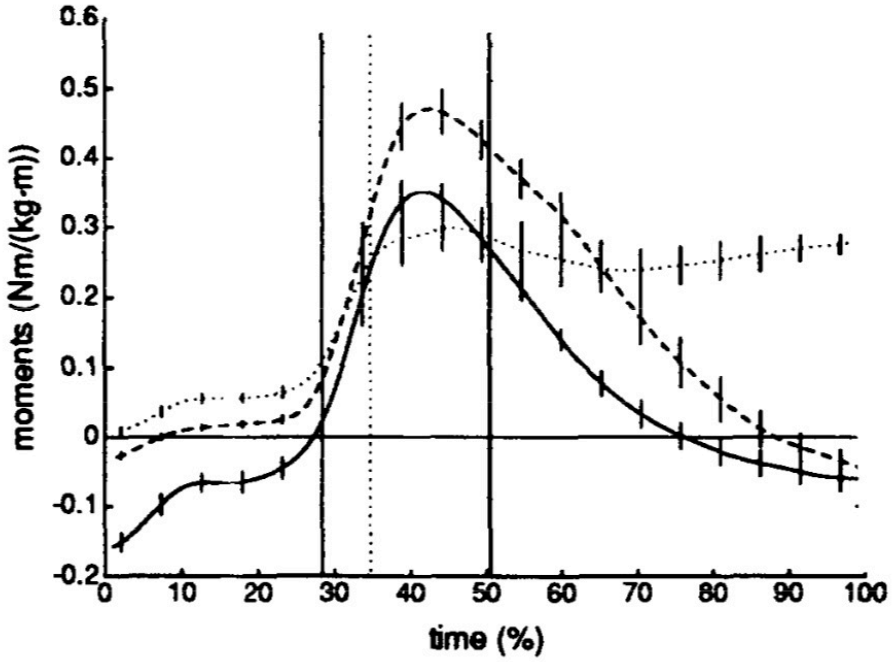

Figure 2.6: STS joint moment data in Nm/(kg-m)(mean height 1.76 m) presented in Roebroeck (1994) (hip-solid, knee-dashed and ankle-dotted)[3]

Based on figures 2.4, 2.5 and 2.6, we can gather the maximum recorded values for knee angle, velocity and torque, and apply them to define the maximum requirements of an assistive exoskeleton knee joint for STS.

2.1.2 Stair Ascent and Descent

Stair navigation is a routine task that requires large physical demands, sometimes even reaching peak joint torques of three times that of normal walking [5]. In order to achieve these physical requirements, elderly individuals often employ alternative strategies to operate within their capabilities. Reeves (2009) characterizes these strategies as typically applying joint moments differently across the knee and ankle in efforts to deload higher stressed joints; usually resulting in higher ankle and lower knee torques [16]. In order to build an effective exoskeleton, it is helpful to examine previous literature on the stair navigation patterns of both elderly and young individuals. In this section we will review a few of the studies conducted to gather knee joint biomechanical data during both stair ascent and descent [5,16,17,34,35].

Stair ascent requires predominantly concentric muscle strength as the body is lifted up [5]. As aging occurs, concentric strength tends to decline, especially for knee extensors, thus the need to reduce or redistribute moments among joints [16]. The strategies that have been presented apply joint moments in such a way that energy is translocated from the knee to ankle, increasing ankle moment at maximum demand and enabling plantarflexors to act over a more favorable portion of the ankle joint moment [16]. For the purpose of better understanding these strategies and their overall effect on human motion, studies have been conducted on joint moment, ROM and velocity for participants throughout the stair ascent movement [5,16,35,34]. Data from these studies are presented in table 2.2.

Parameter	Young adults	Elderly adults
Range of Motion(deg)	5-95 [5] 4.5-86.1 [35] 14.5-94.2 [16]	16-95.6 [16]
Torque(Nm/kg)	1.1 [5] 1.29 [35] 1.19 [16] 0.92 [34]	0.89 [16]
Velocity at Maximum Moment (rpm)	19.91 [16]	19.28 [16]

Table 2.2: Stair Ascent biomechanical data collected from literature for young and elderly adults (0°= straight leg)

The data presented in table 2.2 will be used for determining the requirements of the exoskeleton. Reeves (2009) presents data on elderly participants climbing stairs and finds a ROM of 16-95.6°, a maximum torque of 0.89 Nm/kg and velocity of 19.28 rpm [16]; showing that the knee moment, full degree of extension and velocity have all been reduced in elderly participants.

Compared to stair ascent, descent has been found to produce even greater torques at the knee. Due to a combination of possessing a lower maximum force capability and the large maximum moment it takes to lower the body during stair descent, the elderly must operate much closer to their physical capacities. Operating closer to physical limits can result in less dynamic balance control, meaning a more unpredictable and dangerous descent, along with increased risk of injury [17].

Biomechanical data from literature is presented in table 2.3. Once again it can be observed that elderly participants produced less joint torque and move at slower speeds during stair descent. Out of all the ADL discussed in this thesis, it was observed that stair descent required the largest average knee torque and thus represented the maximum requirements of an assistive exoskeleton. Figures 2.7 and 2.8 present graphical data of the knee moments and angles for ascent and descent compared to level walking [5].

Parameter	Young Adults	Elderly Adults
Range of Motion(deg)	18-90 [5] 12.7-91.8 [17]	12-90.2 [17]
Torque(Nm/kg)	1.45 [34] 1.4 [5] 0.91 [17]	0.83 [17]
Velocity at Maximum Moment (rpm)	34.93 [17]	23.83 [17]

Table 2.3: Stair Descent biomechanical data collected from literature for healthy, young adults (0°= straight leg)

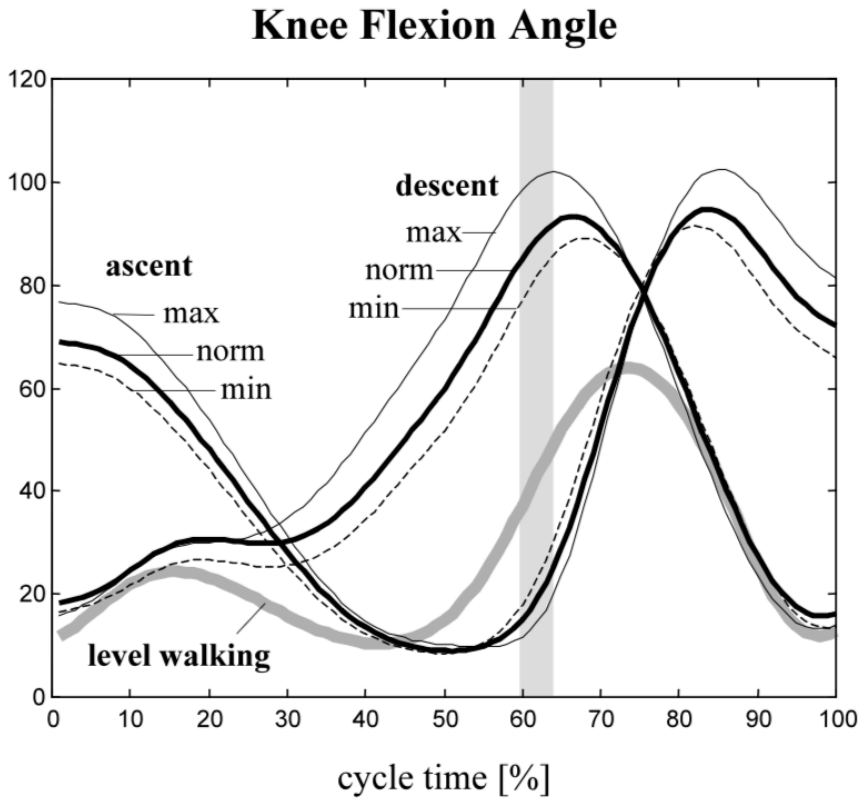

Figure 2.7: Knee angles during Stair ascent, descent and level walking [5]

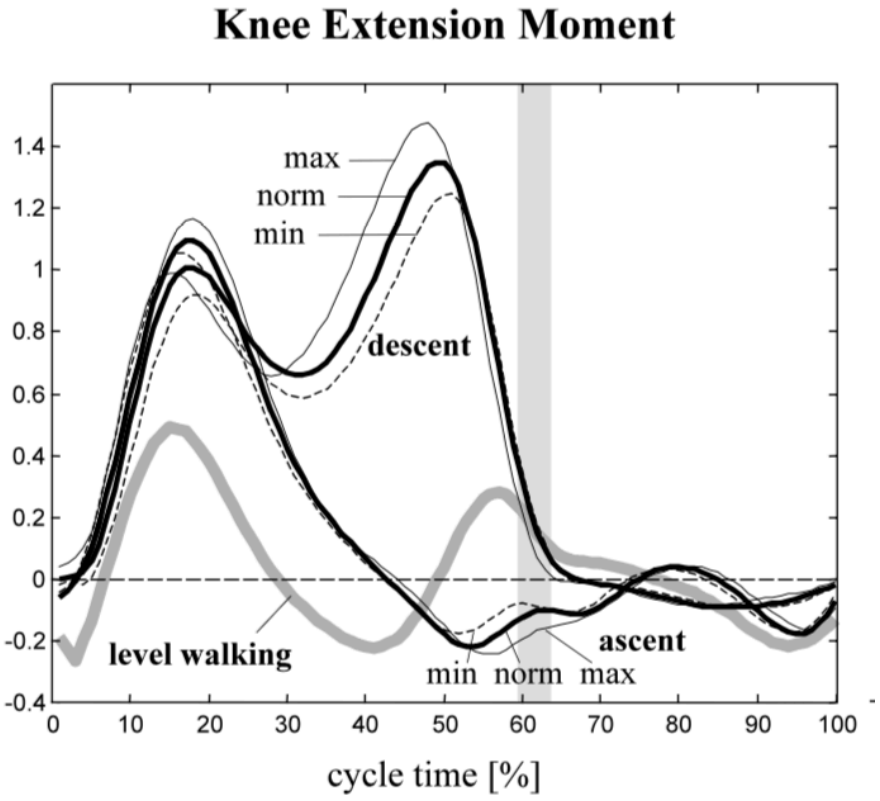

Figure 2.8: Knee moment during Stair ascent, descent and level walking [5]

2.1.3 Hill Ascent and Descent

Often farm lands have rugged terrain that must be traversed throughout the work day. In order to traverse these lands and get to crops, farmers must navigate hills daily. This task is no easy feat for elderly individuals because the physical requirements of hill navigation are similar to that of stair navigation. Studies conducted on hills focus on the effects of inclinations on joint mechanics during walking and quantify the biomechanical values typically observed throughout movement [6,36,37]. Figures 2.9 and 2.10 from Lay (2006) present knee angle and moment data for inclines at -39%, -15%, 0%, 15% and 39% [6]. Analysis of figures show that as incline becomes steeper, physical requirements of hill navigation increases.

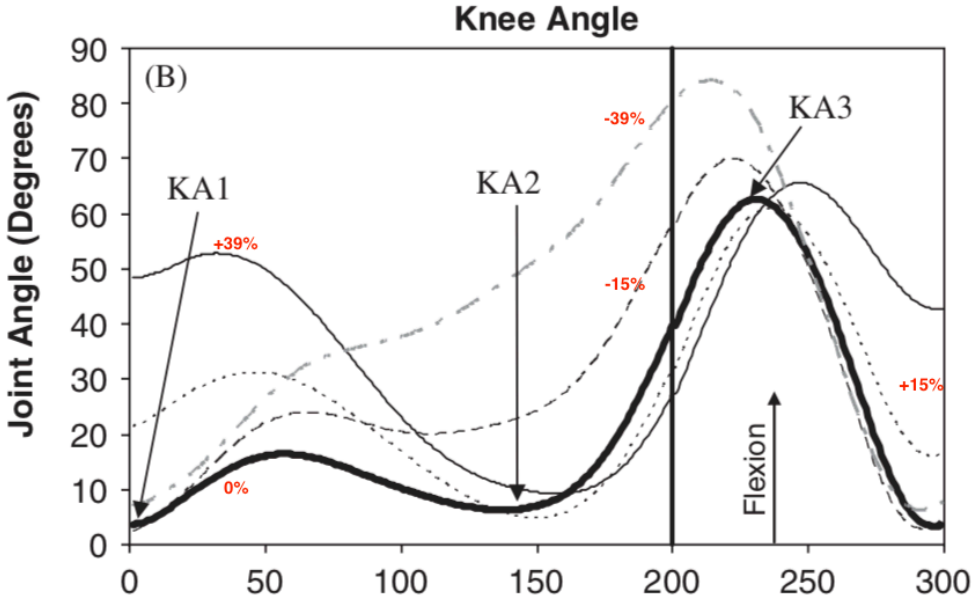

Figure 2.9: Knee ROM for inclinations of +39%,+15%,0%,-15%,-39% (KA1=angle at heel strike, KA2=angle at 75% stance, KA3=Maximum Swing Flexion) [6]

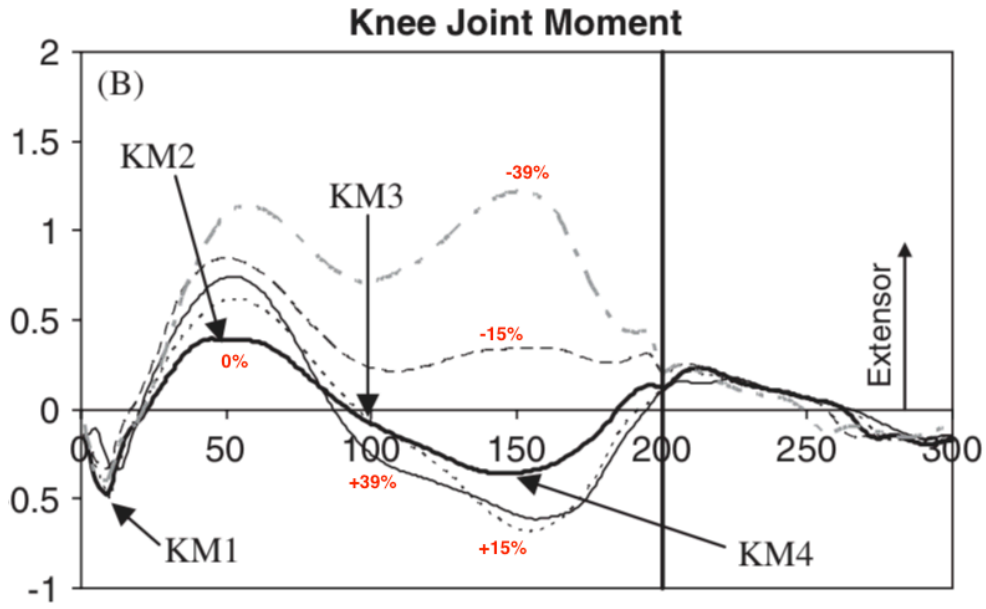

Figure 2.10: Knee Moments (Nm/kg) for inclinations of +39%,+15%,0%,-15%,-39% (KM1=Maximum Flexor Moment, KM2=maximum extensor moment in early mid-stance, KM3=value at 50% stance, KM4=maximum extensor moment in late stance)[6]

2.2 Exoskeleton Review

As the population ages, interest in developing methods to assist elderly in their ADL increases. Exoskeletons provide assistance to wearers by relieving loads or augmenting the capabilities of the wearer. Active exoskeletons in particular are capable of providing large amounts of assistance due to their reliance on powered actuation and sensing. Through research, engineers have been creative enough to develop several methods of powered actuation including hydraulic [38], pneumatic [39], direct drive electric motors [40], series elastic actuators (SEA) [12] and Bowden cable driven systems [8,9,41]. All of these systems have their advantages and disadvantages but for the sake of this review, we will focus on previously developed exoskeletons most related to the one proposed in this thesis by either mechanism or application.

There are many knee exoskeletons that have been developed or are currently being developed.

One example of such an exoskeleton is the quasi-passive knee exoskeleton for investigation of motor adaptation of lower extremity joints [7]. This exoskeleton replicates the spring-like behavior of the knee joint during stance through an external spring and clutch system. The clutch system is controlled through force switches located at the heel and toe, triggering engagement and disengagement of an assistive spring. The quasi-passive knee exoskeleton is designed to demonstrate two levels of stiffness and assist the knee joint with an external parallel spring during the weight acceptance phase of the gait cycle. The exoskeleton is comprised of a thigh segment which includes a stiffness control module (SCM) and thigh cuff and a shank segment including a pulley, potentiometer and shank cuff as shown in figure 2.11 [7]. The SCM controls engagement of the return spring and assistive spring. Once triggered by foot switches, the SCM engages the assistive spring by a friction-based latching mechanism. A steel tendon wrapped around the shank pulley rotates together during knee flexion and pulls the shaft of the SCM that in turn converts the linear stiffness of the engaged assistive spring and return spring into a torsional stiffness around the knee joint allowing assistance to be provided [7]. Preliminary results show that the exoskeleton can provide high torques to the knee joint without notably affecting the kinetic and kinematic behaviors of the wearer [7].

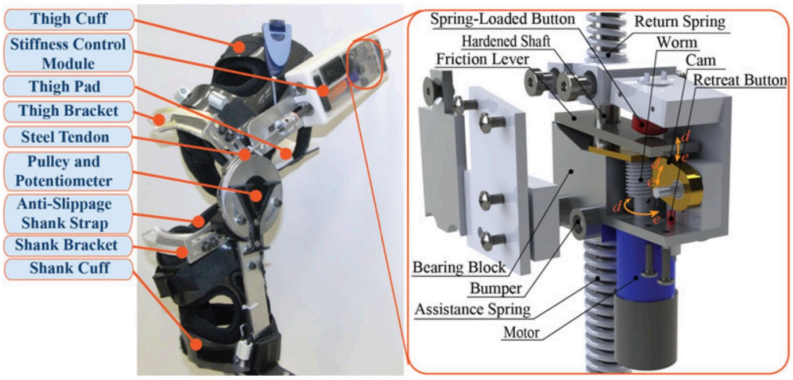

Figure 2.11: The design and structure of a quasipassive knee exoskeleton used to investigate kinetic and kinematic behavior of the knee joint when assisted by a spring in parallel [7]

2.2.1 Bowden Cable Driven Systems

Bowden cable systems have been employed in exoskeleton development due to their ability to reduce mechanism weight and metabolic cost through actuator relocation while still remaining relatively simple. In a cable transmission system, a cable is guided within in a flexible sheath from a powered actuator to the robotic joint. Remote joint actuation occurs when mechanical power from the actuator is delivered to the joint by displacement between the cable and outer sheath, resulting in an applied force in the joint causing actuation[41]. Actuators for these systems are usually DC motors because they allow for easy relocation, fine speed control and regulation, high efficiency, high power to weight and ability to quick start, stop or reverse. Three examples of cable driven systems from previous literature are discussed in this section.

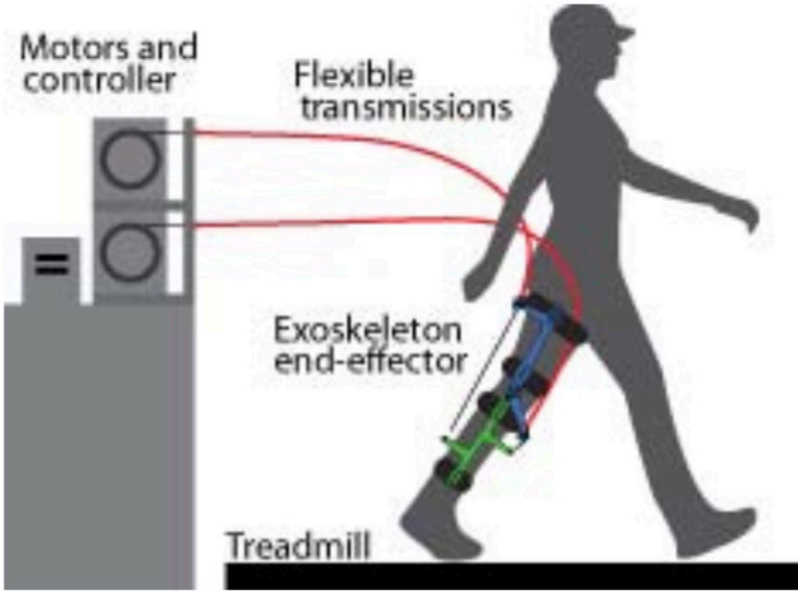

Figure 2.12: Tethered Exoskeleton developed at Carnegie Mellon University [8]

Figure 2.12 from Witte (2017), presents a tethered, torque-controlled knee exoskeleton developed at Carnegie Mellon University[8]. It was designed to assist in gait rehabilitation for individuals with chronic gait abnormalities due to injury, stroke or other illness. The exoskeleton uses two off board servo motors and a real time controller to transfer mechanical power to the human interface by pulling Bowden cables that are routed throughout the exoskeleton structure resulting in walking assistance. Due to the presence of two cables, one along the anterior of the exoskeleton and the other along the posterior, it is able to assist both flexion and extension. The frame is made of carbon fiber struts that are located on the medial and lateral sides of the legs, providing a strong and lightweight frame. The Bowden cable is passed from a cross bar located on the front of the thigh section of the exoskeleton to the calf section. Tension in the cable provides an extension force that creates a torque and acts on the wearer through the straps located on their upper thigh, lower thigh, calf and ankle. In order to work in conjunction with the wearer, an encoder is used to detect knee angle, foot contact is detected with heel switches and strain gauges are used to determine force in the cable and ultimately detect torque based on geometry. Using these sensing methods they are able to develop a method combining proportional control, damping injection and iterative learning to control exoskeleton torque [8].

Another example presented in figure 2.13, is a cable driven exosuit, which relies on soft interfaces to apply forces to the wearer at the hip and ankle joints [9]. This exosuit provides assistance during walking by applying force to ankle plantarflexion, hip flexion through a multiarticular load path and hip extension through a separate load path. Assistance is created by making use of joint synergies in timing, with one motor actuating the multiarticular path for both legs and another motor actuating hip extension for both legs. Transmission of forces is accomplished by Bowden cables originating at proximate mounted motors and guided through specific pathways on the suit. Control is based on force profiles that use

Figure 2.13: Cable driven Exosuit for assistance in walking of up to 4 mph[9]

biological joint torque and works in conjunction with encoders at the motor, gyroscopes at the heel and load cells at Bowden cable termination points. The gyroscopes detect foot contact and identify a pattern within the step to determine the gait cycle. Load cells were used to monitor suit tension and calculate torque applied to the joint. Based on feedback from the sensors, a force-based position control is developed and used to provide 21% and 19% of nominal biological moments at the ankle and hip during normal walking [9].

The AssistON-Knee exoskeleton presented by Celebi et al. is an assistive device used to aid flexion/extension of the knee, while also accommodating knee translational movements [10]. It has the ability to self-align the human and exoskeleton knee axes due to a custom made planar parallel mechanism, guaranteeing shortened set up time, ergonomy and comfort throughout therapy. An under-actuated Schmidt-coupling is implemented to allow active

control of knee rotation but also allows passive translation of the exoskeleton axis throughout knee movement. The coupling connects the thigh and shank components of the exoskeleton and the input drive is actuated through the use of a Bowden cable series elastic actuator. This enables the actuation unit (figure 2.14) to be placed away from the knee, reducing the weight of the knee exoskeleton. The actuation unit is composed of a 200W brushed DC motor and 1:50 reduction ratio to deliver up to 35.5 Nm of continuous torque. A commercial knee brace is used to attach the exoskeleton to the thigh and shank of the patient (figure 2.14). Electromyography (EMG) results gathered from testing of the exoskeleton show that it is effective in decreasing effort required for extension during STS [10].

Figure 2.14: AssistON-Knee and remote actuation unit [10]

2.2.2 Exoskeleton for Sit to Stand

STS is an extremely difficult task for individuals who have suffered from stroke. In particular STS is characterized by postural sway and weight bearing imbalances between paretic and unaffected legs, leading to increased falls [42]. Sheperd (2017) presents the design of a STS active knee exoskeleton to assist mobility challenged individuals [11]. The exoskeleton is designed to produce the full torque required of STS, be torque controllable with appropriate bandwidth, minimized weight, minimized lateral protrusion and appropriately transmit forces from exoskeleton to person without creating torsion or axial twisting about the thigh. Actuator design is composed of a brushless DC motor driving a lead ball screw with a ball nut that is linked to a fiberglass beam spring through a two force member. The spring is attached to the lower segment of exoskeleton and when force is applied to it in a cantilever manner it causes rotation about the knee joint. The choice to include a spring in this design allows for accurate measurement of torque by measuring spring deflection, finer control, extremely high energy storage capacity and improving backdrivability by allowing more time to make adjustments to positional perturbations [11]. Two levels of controllers are implemented. A high-level controller used to determine desired torque of the exoskeleton based on a torque-angle relationship and a low-level controller that attempts to accurately track a desired torque [11]. Figure 2.15 shows the component makeup and structure of the exoskeleton actuator.

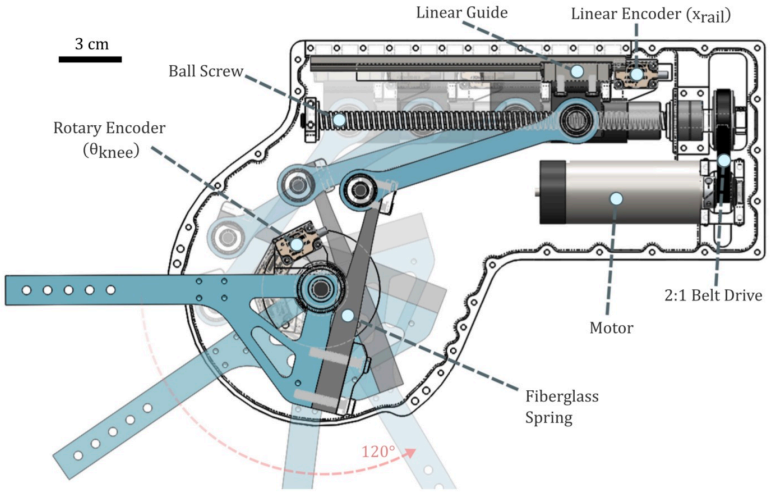

Figure 2.15: STS actuator structure and method of actuation [11]

The exoskeleton presented in Junius (2014) is designed to assist with STS movements by providing forces at the hip, knee and ankle [12]. It builds upon an existing brace to improve wearability and uses a SEA mechanism consisting of pulleys, springs and cables to provide joint actuation. The mechanism works by driving a motor and small pulley located at the upper thigh, which in turn is connected to a larger pulley with a lever arm located at the knee. As the position of the lever arm is set by the motor, a cable connected to both the lever arm and a spring is pulled, thus compressing the spring to store energy that can then be applied to the joint to provide an assistive torque. The amount of assistance is determined by an assistance-as-needed strategy where active participation of the user is encouraged; meaning that the assistance provided is based on the amount of force the user is unable to produce, hence covering the capability gap between the user and biomechanical requirements of the task. Controls to better assist the wearer will be developed based on two encoders, one optical to detect the angle between upper and lower link of the exoskeleton and an absolute to determine the angle between the lever arm and upper link[12]. Figure 2.16 depicts the STS exoskeleton.

Figure 2.16: STS Exoskeleton using SEA mechanism [12]

The Myosuit is another example of a soft wearable device. It is designed to provide continuous assistance at the hip and knee joint when working with and against gravity in ADL, in an effort to aid individuals suffering from muscle weakness [13]. The device combines active and passive elements with a posture-based force loop controller to behave as an external muscle and provide gravity compensation to the wearer. It delivers support to the wearer's hip and knee joint through the use of a system of soft textiles, rubber bands, dyneema cables and actuation units. Testing of the device during STS action shows that the suit and control combination are capable of successfully identifying changes in posture and assist hip and knee extension moments up to 26% and knee power up to 35% [13]. Figure 2.17 presents the Myosuit structure.

Figure 2.17: Component structure of the Myosuit used to assist individuals suffering from muscle weakness [13]

2.2.3 Exoskeleton for Stair Climbing

Currently, designing exoskeletons for stair navigation have proven to be a tough challenge for researchers because of the task's demanding biomechanical requirements. One example of such an exoskeleton, is the one designed at Vanderbilt University to help paraplegic individuals succeed in climbing and descending stairs[14]. The exoskeleton makes use of direct drive brushless DC motors to actuate the hip and knee through gear reduction transmissions. In combination with a stability aid, the exoskeleton works to estimate the wearer's center of pressure and use the distance between that center and location of the forward ankle joint as a primary input for assistance control. The act of leaning forward or backward indicate user intention and are used as reference points within the gait cycle, so that the exoskeleton can determine the timing and level of assistance necessary to best aid the wearer. Figure 2.18 shows the Vanderbilt Exoskeleton being used to assist an individual ascend stairs[14].

Figure 2.18: Stair negotiation exoskeleton developed at Vanderbilt University to assist paraplegic individuals [14]

Chandrapal (2013) presents an actuated lower limb exoskeleton intended to provide gait assistance by supplying supportive torques at the knee during stair climbing [15]. The exoskeleton prototype was manufactured from carbon fiber to fit precisely on a test subject. It produces assistive torques for extension and flexion through the use of pneumatic artificial muscles, two for flexion and two for extension. The artificial muscles are capable of producing a maximum force of 150 N. In addition to mechanical mechanisms, a control structure to monitor and direct exoskeleton actuation was developed. An adaptive fuzzy controller that uses error signal based on torque feedback, and an intention estimation algorithm based on muscle activation and joint angle to adapt to plant and improve corresponding action is implemented. The output varies the pressures within the artificial muscles to produce a desired force. Surface electromyography (sEMG) were used to collect data on muscle contraction and placed at five major muscles that flex and extend the knee.

Test were conducted on a healthy individual over ten days to determine if exoskeleton assistance reduces muscular effort and if the method used to estimate user intention affect fluency and effectiveness of assistive torque. Testing was conducted under three different estimation algorithms, Multilayer Perception (MLP), linear and nonlinear algebraic functions. Results

show the exoskeleton was most effective in reducing muscular effort during stair climbing when using MLP, with reductions of peak activation in four out of five muscles, in particular reducing biceps femoris by 52%. An important deduction from the testing of this device showed as assistance increased, metabolic cost increased and unnatural and stiff movement were more prevalent [15]. Figure 2.19 shows exoskeleton hardware and data flow [15]. Figure 2.20 shows the block diagram for the control structure supporting exoskeleton performance [15].

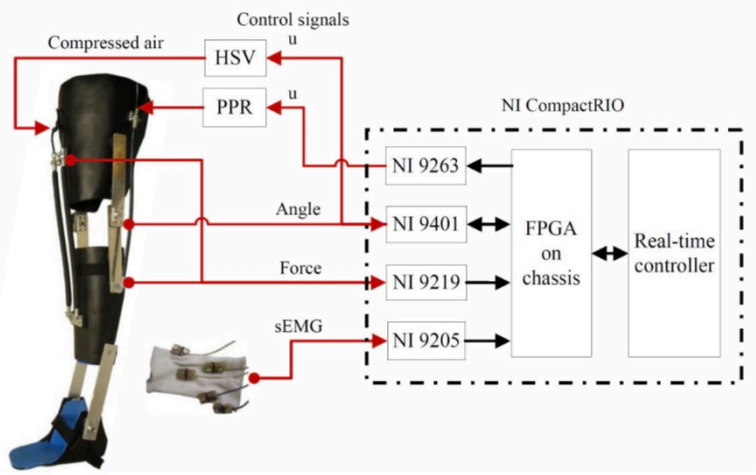

Figure 2.19: Pneumatic Exoskeleton used for providing assistive torque for stair climbing hardware and dataflow [15]

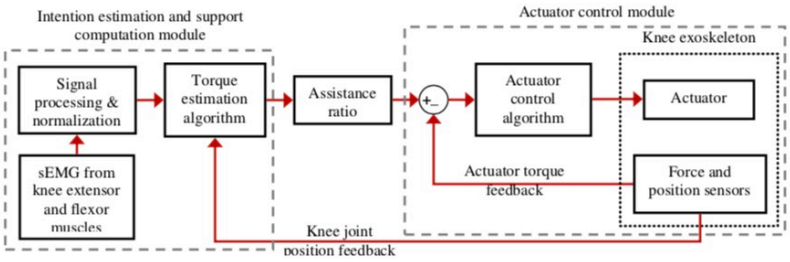

Figure 2.20: Block diagram of control structure used in pneumatic exoskeleton for assistance in stair climbing [15]

Chapter 3

Design Goals

As previously discussed exoskeletons are wearable devices designed to interact with and provide assistance to their wearers. Such a device has many criteria that must be first established for its design and development. The criteria can be divided into the categories of wearability and mechanical capability. Wearability requirements include limitations on weight and form factor, it must be comfortable, have full ROM and is easy to use. For example, in a farming environment it is necessary for wearers to navigate small areas and interact with machinery. In order to minimize possible interference with the surrounding environment, form factor must be minimized. Another example is weight and comfortability criteria which become very prevalent in devices used for extended periods of time. A heavy device will typically be more harmful than helpful to its wearer and an uncomfortable device will not be worn for very long, thus being of no use to those it is aiming to assist. Full ROM is necessary so that the wearer does not feel restricted and is able to perform all of their intended actions without resistance. A typical range of motion is from 0° to 135° with a flexion angle of 125° being the angle at which most normal activities can be performed [43]. Table 3.1 shows the maximum flexion values required to perform everyday movements.

Task	Max Knee Flexion
Walking	65°
Lift Object from floor	70°
Stair Ascent	85°
Sit and stand comfortably	95°
Tie shoelaces	105°
Squat	115°

Table 3.1: Max knee flexion for everyday movements (0° = fully extended)

Taking into consideration wearability criteria, we established several design goals for the knee exoskeleton. The exoskeleton will weigh less than 4 kg total to mitigate any excess inconvenience during extended use and will extend less than 5 inches from the side of the leg, reducing the chance of collision with surrounding environment. It will have a range of motion from 0° (full extension) to 115° (flexion), allowing the wearer to perform any task from straightening their leg to squatting. In addition to full ROM, the exoskeleton will be backdrivable allowing for wearer driven movement. backdrivability creates high force sensitivity and high impact resistance allowing quick adaptation to external forces and is beneficial for human-robot interaction. Soft interfaces such as leg pads and a waist belt will be used in human-exoskeleton interaction in an effort to increase comfortability, allow for compliance and prevent unwanted exoskeleton shifting while worn. Finally, the exoskeleton will be able to be donned in less than two minutes.

The second group of criteria focus on mechanical capabilities of an exoskeleton. Criteria are based on the torque, speed and angle of human motion patterns. The data taken from literature review can be used to define required exoskeleton torque, speed, actuation range of motion and control requirements that are best suited to provide assistance to a wearer. Angle and torque data are digitized from literature review and presented in figure 3.1. Maximum velocity requirements are shown in table 3.2. Data is acquired from literature review of Roebreck (1994), Riener (2002), Lay (2006), Reeves (2008 and 2009) [3,5,6, 16, 17].

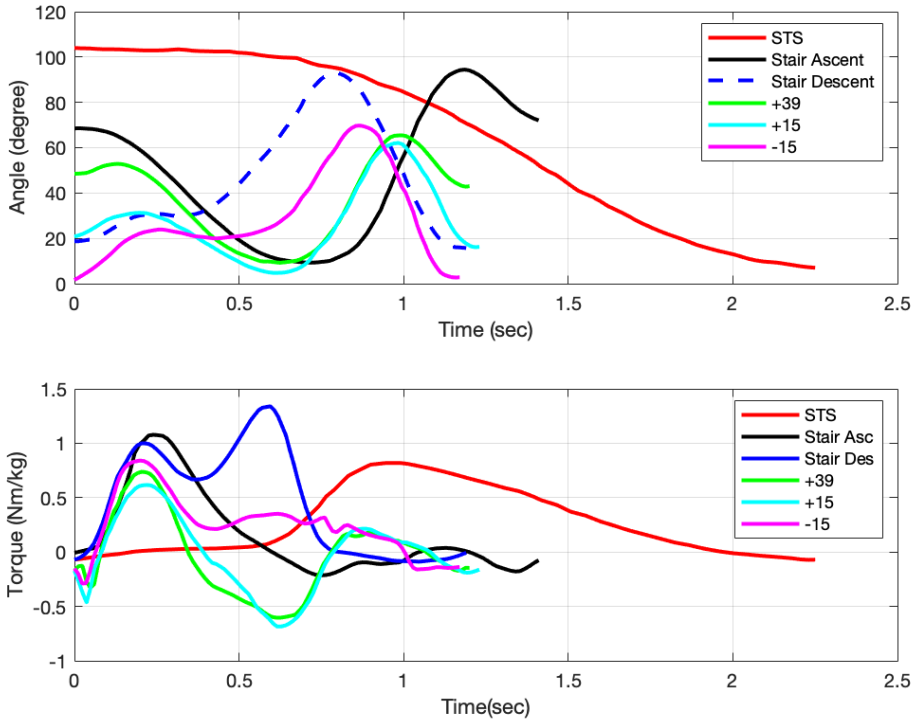

Figure 3.1: Biomechanical Angles and Torque profiles during STS, Stairs and Hill negotiation. (0° = full extension) [3,5,6, 16, 17]

Task	Maximum Joint Velocity (RPM)
STS	14.14
Stair Ascent	50.24
Stair Descent	48.59
Hill Ascent	42.17
Hill Descent	57.66

Table 3.2: Maximum knee anglular velocity from Literature (0° = fully extended) [3,5,6, 16, 17]

Gathered human biomechanical data shows that the target ADL have a range of motion from 0° to 105°, a peak torque of 1.35 Nm/kg and peak joint velocity of 57.66 rpm. Applying this data along with other information acquired from literature review, we established the following mechanical goals for the design of an active knee exoskeleton. The first goal was the exoskeleton's ability to provide at least 30% of the required maximum torque of all intended

activities. Using 80.7 kg, which is the average mass of a North American adult [44], the required peak exoskeleton torque was calculated to be 32.7 Nm applied at the knee. 30% was chosen based on the studies of strength and muscle loss with age and the effect of excess assistance on muscle loss [45,46]. Keller (2013) studied the effect of strength and muscle loss with age and concluded muscle strength declines 16.6-40.9% in people older than 40 and that the most profound changes in muscle loss begin occurring after 50 [45]. It was found that there is a 1-2% per year loss of leg mean body mass and 1.5-5% per year strength loss reported in individuals older than 50 years old [45].

The second paper taken into consideration studies the effect of muscle weakness on the capability gap, i.e. the difference between the strength of the individual and task requirements [46]. The study's goal was to calculate the capability gap when muscle weakness is present and translate those findings to the design of exoskeletons. Often exoskeletons are designed to provide excess amounts of assistance than necessary, ultimately resulting in wearer muscle atrophy due to disuse and exoskeleton overreliance. In order to avoid causing muscle atrophy, it is recommended to employ an assistance as needed strategy (AAN), which suggests that assistance is provided to only cover the capability gap between task requirement and wearer capabilities [46]. We took considerations from both papers and chose up to 30% of maximum torque assistance. This value covers 50th percentile of strength loss found in individuals over 50 without creating excess reliance on the device for ADL.

Our next goal was to design an exoskeleton capable of moving at velocities similar to that of biomechanical requirements. As shown earlier these velocities range from 0 - 53.64 rpm. In order to account for variance in gait patterns, we aimed to design our actuator with a safety cushion and thus set our desired speed capabilities at 75 rpm. Our final goal was to implement an angle-based torque control system capable of varying assistance based on knee angle as STS is performed. An angle-based torque controller is a low level controller that

is utilized to ensure the exoskeleton provides a specific level of assistance based on the STS torque-angle relationship that has been reviewed through literature. An effective controller will minimize improper human-exoskeleton interaction, while maximizing the effectiveness of assistance provided.

Goal	Reason
Full ROM	Allowing wearer to perform all normal activities without resistance
weighs less than 4kg	Prevent putting excess strain on the wearer due to large amounts of weight
Minimized Volume	Minimize interference with surrounding environment
Soft interface between human and exoskeleton	Increased comfortability during human-exo interaction
Backdrivable	Beneficial to human-exo interaction by creating quick adaptability to external forces
Prevention of unwanted shifting on leg	Increases comfortability as exoskeleton is worn for longer periods
Donned in two minutes	Not a hassle to put on and wear
Produce 30% of joint torque	Provides a reasonable amount of assistance to cover capability gaps without creating an overreliance
Capable of matching joint velocity	Allows wearer's natural motion profile movement
Implementation of low-level controller for task performance	Controls exoskeleton performance to provide the most effective assistance

Table 3.3: Design Goals

Chapter 4

Exoskeleton Design

4.1 Overview

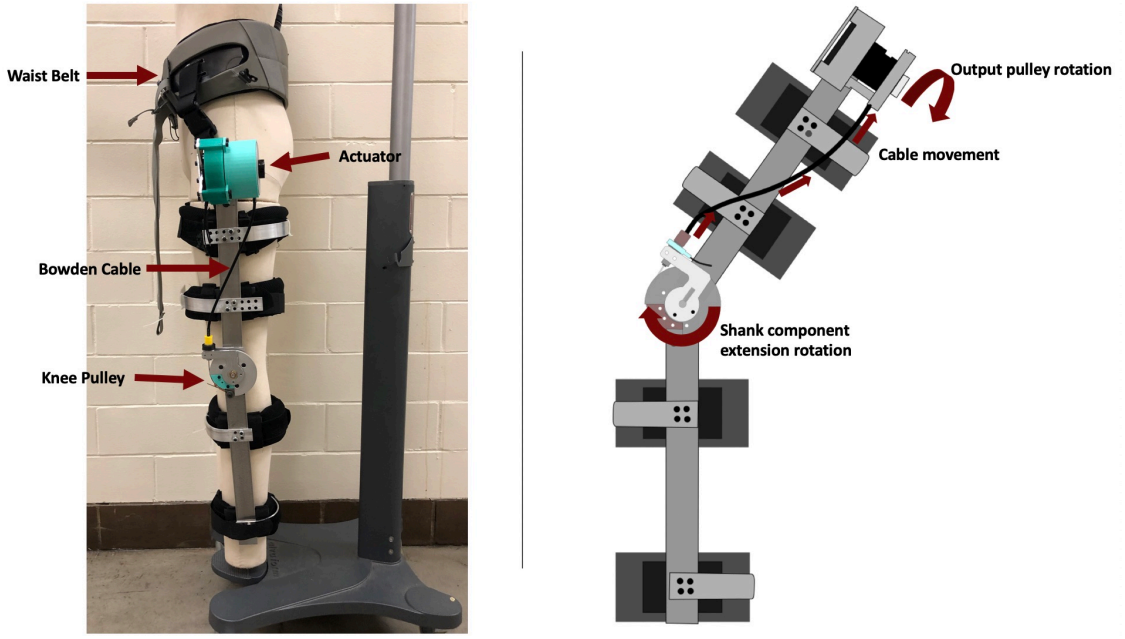

Figure 4.1: Active knee Exoskeleton as fitted and intended mechanism of operation depiction

The designed active knee exoskeleton, figure 4.1, is a Bowden cable driven wearable device that provides extension moments at the knee joint in order to assist in performing ADL. The exoskeleton can be categorized into 3 subsystems: (1) a human interface, which interacts with the wearer to transmit forces provided by the exoskeleton, (2) an actuator unit which supplies the desired torque for assistance, and (3) an electronic subsystem which drives

and monitors exoskeleton performance throughout it's operation. The human interface is composed of an aluminum frame, pulley for joint actuation, four soft thigh cuffs located along the leg, four aluminum supports located at the thigh cuffs to aid in the transmission of forces and a waist belt to assist in keeping the exoskeleton in place. The actuator module is located at the hip to minimize the effects of distally placed mass and is connected to the knee through the use of a Bowden cable. It consist of a brushless DC motor (BLDC), a two stage planetary gearbox (Vex Robotics VersaPlanetary), aluminum frame and output pulley. Electronic components include incremental encoders located at the knee joint and behind the motor, a load cell, microcontroller, motor controller shield, instrumentation breakout board, load cell amplifier and programmed angle-based torque controller. These three subsystems work cooperatively to provide assistance to the wearer and operates as described below.

A joint angle is read by the knee incremental encoder, the microcontroller refers to a specific equation dependent on the range the measured knee flexion angle falls within and calculates a desired level of torque accordingly. The torque is converted into a corresponding current to be fed to the motor. Motor torque is generated, which is then amplified by gearbox ratio and a torque is generated at a pulley located at gearbox output. As the pulley rotates the attached Bowden cable is pulled upwards resulting in a force that acts on the outer radius of the pulley at the knee creating a joint moment. The exoskeleton joint moment is then translated to normal forces applied to the wearer through interaction with the four thigh cuffs of the human interface. The applied forces provide an assistance to the extension moment produced by the human joint and result in easier movement to desired position.

4.2 Actuator

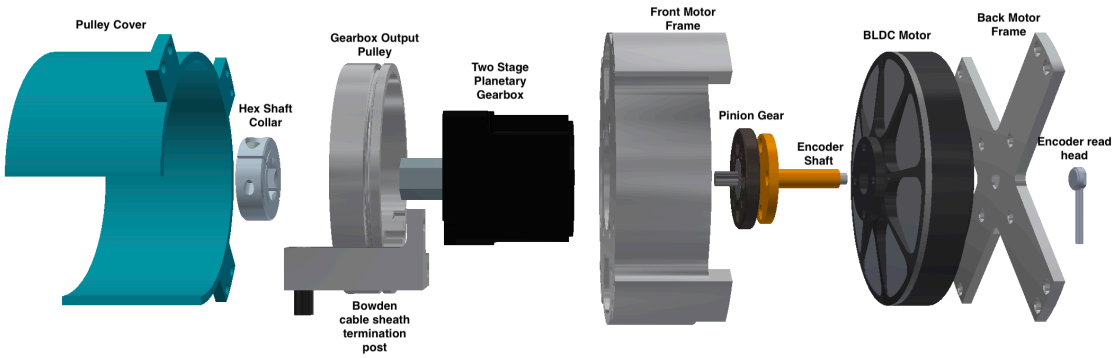

Figure 4.2: Exploded view of actuator components

The actuator is responsible for producing an assistive joint torque that is used to help the wearer throughout task movement. It is composed of a BLDC quadcopter motor (T-motor U8 lite), a two stage planetary gearbox (Vex Robotics VersaPlanetary Gearbox) with a 25:1 reduction, pulley at gearbox output and a supporting aluminum frame, as shown in figure 4.2. Design prioritized the following considerations: biomechanical task requirements, metabolic cost of wearing the actuator (mass and location), module volume, safety and reliability. In this section the actuator design and process is further described.

As mentioned earlier, an actuator's allowable mass, output torque and required speed are determined by the application. These requirements still leave a broad design space in which to select method of actuation, motor size and gear ratio. Our first step was in deciding method of actuation. A key consideration in our design process was actuator mass and location of mass. The location of added mass is important because previous studies have shown that when mass is added to the extremities, lower extremity kinematics can change and metabolic rate increases disproportionately with load, especially in more distal locations [47]. Browning et al. found that a 4 kg waist load did not result in significance increase in net metabolic rate while at 8 kg it increased by 14% and walking with the load located at the

foot increased rates by 48% [47]. Based on this data we aimed to keep the entire exoskeleton below 4 kg and the largest amounts of mass closest to the hip joint of the wearer. These requirements led to design a cable driven system that allows distal actuation. The system is driven by a pulley, and a gearbox and electric motor combination.

4.2.1 Motor and Gearbox sizing

Actuator design began with the selection of a motor. Many types of motors exist such as servo, stepper, brushed and brushless motors. After reviewing these types, a brushless type motor was selected based on several of the advantages associated with using one including high torque to weight ratio, high efficiency, longer lifespan then brushed, less mechanical noise and higher reliability. The motor chosen is the U8 lite KV 100 quadcopter motor from T-motor, figure 4.3. The motor is capable of producing 180 seconds of 2.73 Nm continuous torque at its rated voltage of 44.4 V, weighs 243 grams, no-load speed of 4549 rpm and has a height of 27.05 mm allowing it to be low profile on the side of the body.

Figure 4.3: U8 Lite KV 100 quadcopter BLDC motor from T motor

Although the motor is capable of producing high torques in comparison to other motors, it is still not enough to reach our goal of 32.7 Nm. In order to satisfy our application requirements,

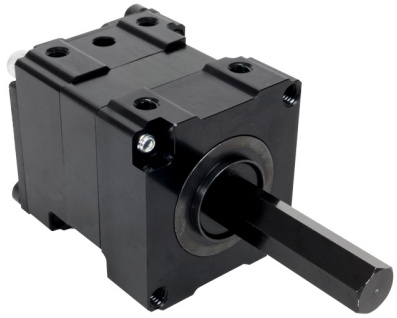

Figure 4.4: VexRobotics VersaPlanetary Gearbox

the motor was paired with a two-stage, 25:1 planetary gearbox that will increase output torque and decrease speed to a value more suitable for our application. Planetary gearboxes incorporate a sun gear that drives surrounding planetary gears within a ring gear thus rotating the output shaft. These gearboxes are advantageous because they provide relatively good efficiency, compact size, low backlash, long gear life due to distribution of forces on multiple gears, easily adaptable and high torque output. The gearbox chosen is a two stage VersaPlanetary Gearbox that provides a reduction of 25:1, figure 4.4. The motor and gearbox combination were then evaluated using motor equations to develop speed-torque, mechanical power and torque-current curves. Performance curves were then compared to application requirements and validated. Motor equations and corresponding graphs are presented below.

$$\omega_m = \frac{V}{K_e} - \tau * \frac{R_a}{(K_t * K_e)} \tag{4.1}$$

Equation 4.1 is used to develop the speed-torque curve of the motor and gearbox. ω_m represents angular velocity, V is voltage supplied, K_e is the speed constant, τ is torque, R_a is resistance and K_t is the torque constant. Speed-torque curve is used to evaluate the expected performance of the motor-gearbox pairing to biomechanical requirements. Figure 4.5 presents curves for both a 12s (44.4 V) and 6s (22.2V) lithium polymer (LiPo) battery.

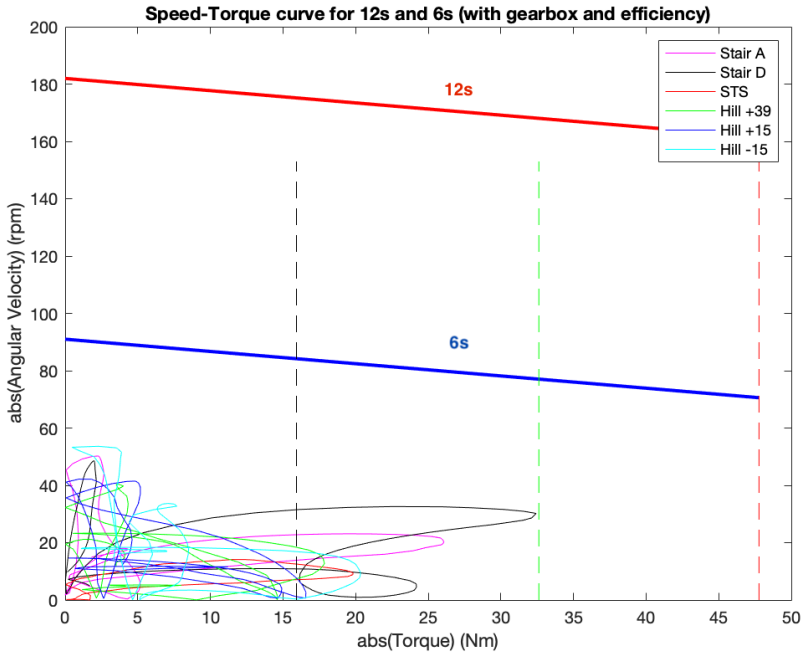

Figure 4.5: Speed-Torque curve for 44.4V and 22.2V. (Vertical lines: Black dashed = nominal torque, green dashed = device current-torque limitation, red dashed = peak 180s continuous torque)

In figure 4.5 absolute values for knee angular velocity and 30% of application torques are presented for STS, stair and hill navigation. These values are compared to motor-gearbox speed-torque curves and presented relative to nominal, peak device and continuous 180s torques. Motor and gearbox output torque is calculated by multiplying motor input torque by reduction ratio and assuming an efficiency of 70% ($\tau_{out} = \tau_{in} * N * \eta$). Nominal torque is equivalent to 15.92 Nm, peak device torque is 32.92 Nm and continuous 180s torque is 47.77 Nm, which can be achieved if amperage limitations of the current device are changed.

Examination of the figure shows that at both voltage levels the gearbox and motor combination provide adequate speed and torque that meet or exceed application requirements. Application torque lines show that the maximum torque requirement occurs in stair descent with a value of 32.28 Nm. As previously mentioned the peak device torque is 32.92 Nm, accounting for efficiency. While the difference between motor-gearbox torque and application torque are small, the 1.15 ratio between pulley at the knee and output shaft pulley will multiply the torque delivered to the joint and create a greater torque cushion. Inspection of speed shows that at the rated battery supply of 12s, there is a large difference between the speed capability of the actuator and joint velocities. Excess amounts of speed is unfavorable to the goal of providing assistance to wearers, as it fails to match natural human biomechanics which may cause wearers to increase effort to match exoskeleton pace and/or resist unnatural movements. In order to combat unnecessary speed, a lower voltage supply was chosen and evaluated. At 22.2V, the speed torque curve is lowered from 180 to 90 rpm at no-load speed. While 90 rpm is still above the maximum joint angular velocity of 53.64 rpm, it creates a much more reasonable speed cushion that will be further reduced by pulley ratio to approximately 78 rpm. This is about the desired speed cushion for choosing a motor and gearbox pairing to be used in this implementation. Selection of a 6s battery also created a weight reduction when compared to a 12s battery.

The next equation is used to calculate mechanical power for both biomechanical data and motor-gearbox combination. Mechanical power (P_m) produced is calculated by multiplying torque and rotational speed as shown in equation 4.2. By utilizing equation 4.2, a power-torque curve can be developed and compared to max power requirements of each motion profile considered in design.

$$P_m = \tau * \omega_m \tag{4.2}$$

Figure 4.6 presents the power-torque curve of the motor-gearbox combination in comparison to peak biomechanical powers. Peak power for biomechanical data is calculated by using equation 4.2 at every angular velocity and torque point throughout the motion pattern then the absolute maximum value is taken and plotted in comparison to the power-torque curve of motor-gearbox.

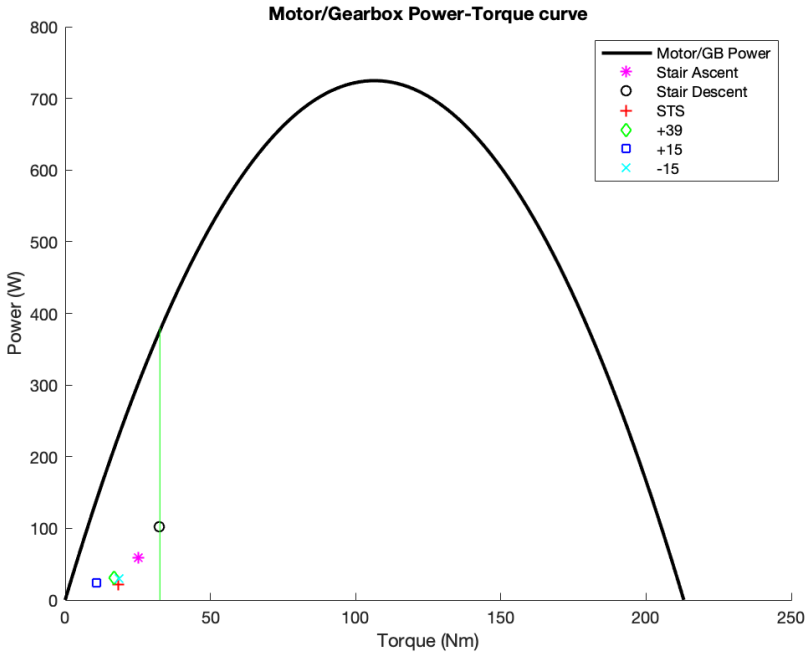

Figure 4.6: Power-Torque curve for 22.2V compared to max power of biomechanical data. (green vertical = device current-torque limitation and peak power of exoskeleton)

Inspection of figure 4.6 shows that the peak power of the actuator is 380 W in comparison to the peak biomechanical power of 102.6 W occurring in stair descent. This reconfirms the assumption generated from evaluation of figure 4.5 that the capability of the designed actuator satisfies joint requirements.

$$\tau = K_t * I_a \tag{4.3}$$

Equation 4.3 is the relationship between torque output and current applied (I_a), which is used to calculate the required current to produce a desired torque. Figure 4.7 shows the linear relationship between current and torque for our selected motor and gearbox. The limitations of current at 20 Amps is due to motor shield selection, which is discussed later in section 4.4.1.

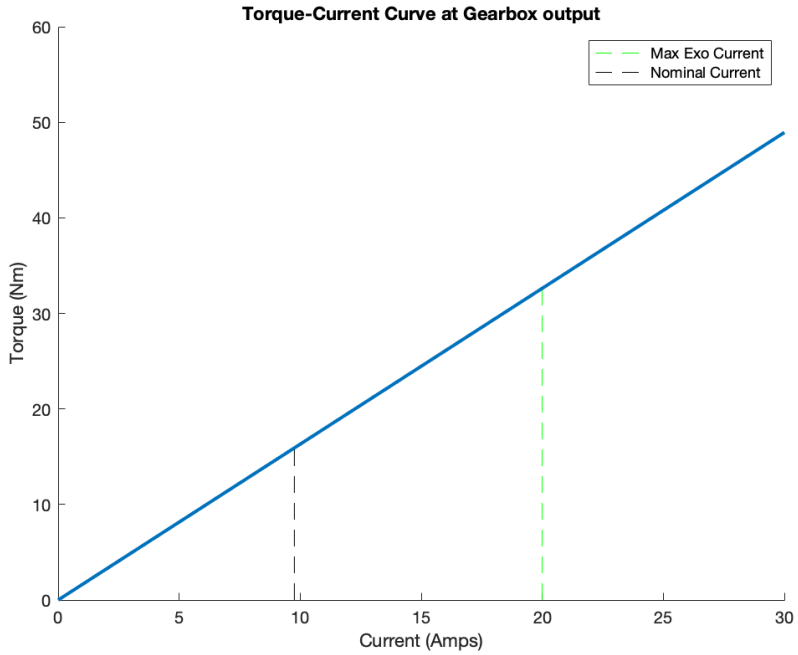

Figure 4.7: Torque-Current curve for motor-gearbox combination (green dashed = device current-torque limitation and peak power of exoskeleton)

Evaluation of all three equations and figures shows the expected performance of chosen motor and gearbox is capable of providing adequate speed and torque to satisfy knee biomechanical requirements.

4.2.2 Pulley design

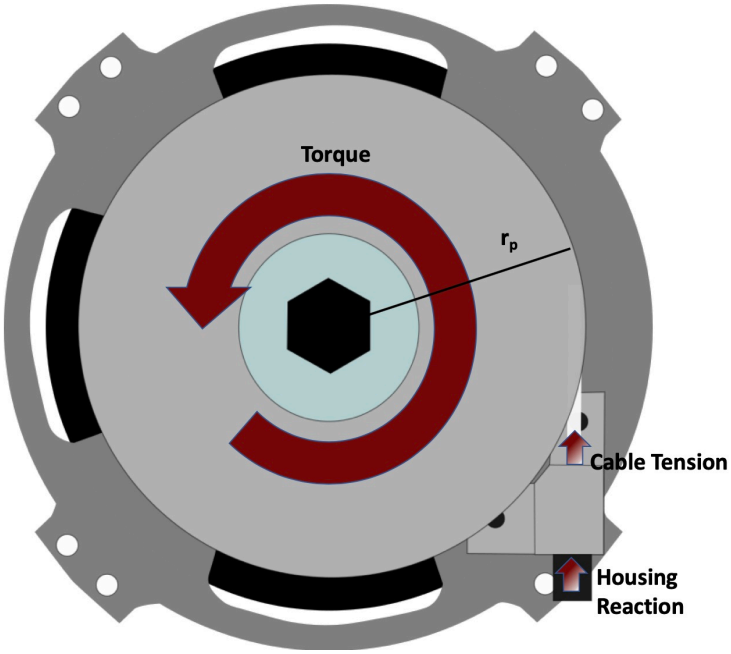

Figure 4.8: Pulley and cable operation

An important element of the actuator is the pulley located at the output of the gearbox. It is press fitted on the hex output shaft of the gearbox and secured with a shaft collar. It's primary responsibility is to facilitate the transmission of torque generated by the motor-gearbox to the exoskeleton joint located at the knee. This is done through a Bowden cable that is mounted to the pulley and secured by a screw as shown in figure 4.9. As the pulley rotates with torque it causes tension in the cable, resulting in a force that is transferred along the cable route to the exoskeleton knee joint, figure 4.8. Force in the cable is calculated by $F_{cable} = \frac{\tau}{r_p}$. Observation of figure 4.9 shows an open cylinder design in the pulley. This is done to ensure that forces from the cable on the pulley are inline with the bearings located in the gearbox, thus limiting shaft loading and deflection.

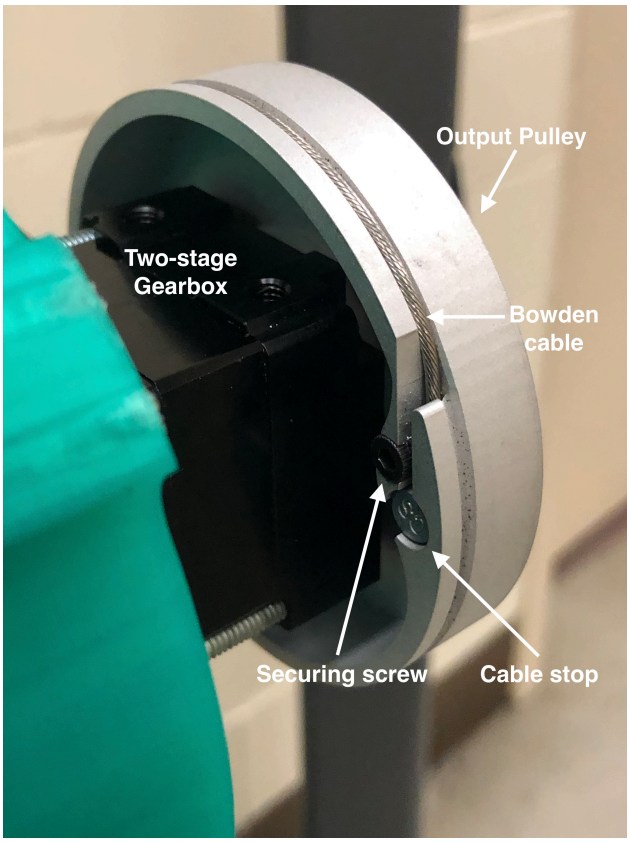

Figure 4.9: Bowden cable attachment mechanism to gearbox output pulley

4.3 Exoskeleton Human Interface

As discussed in section 2.1, the knee joint has six DOF and performs flexion/extension through a sliding and rolling movement between the femur and tibia. Typically, the knee axis of rotation displaces by 8 to 20 mm as the joint flexes [48]. The knee also experiences between 5-10 degrees of external rotation as it extends [49, 50]. In designing exoskeletons to replicate these movements, complex and heavy mechanisms have been developed and implemented. These devices can often present issues in operation or metabolic cost. In order to avoid using mechanisms with large, explicit degrees of freedom, this exoskeleton opts for a simpler method of incorporating compliance between the exoskeleton and wearer into the system. Since knee DOFs outside of flexion/extension involve relatively small movements,

compliance allows the wearer the freedom to perform desired movements without dedicating a specific mechanism or creating excessive resistance. The human interface presented was designed as a single degree of freedom (flexion/extension) exoskeleton that is compliant in all other degrees of freedom.

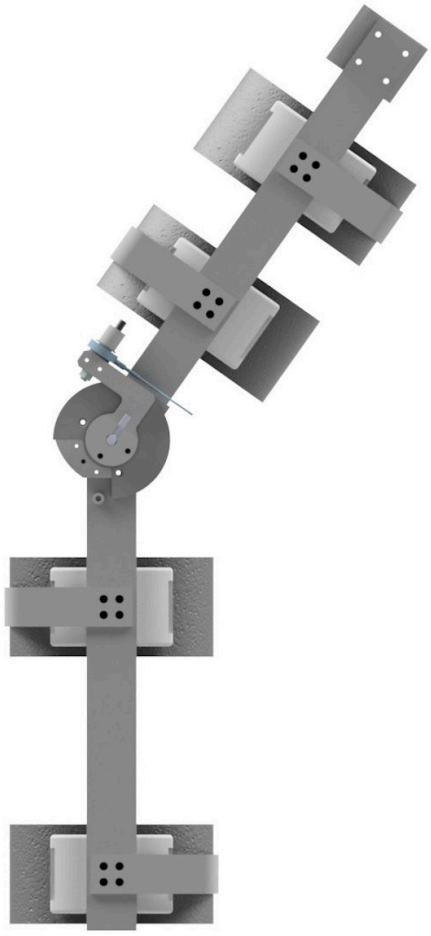

Figure 4.10: CAD model of Exoskeleton end effector that interacts with wearer through four straps at upper thigh, lower thigh, calf and ankle

The human interface (figure 4.10) of the exoskeleton consists of an aluminum frame on the lateral aspects of the leg that can be separated into thigh and shank components. The thigh component is composed of an inner bar that extends from the knee to the hip and an outer support connected to the inner through a crossbar that serves as Bowden cable sheath

termination. The upper thigh component is connected to a waist belt to minimize downward migration of the exoskeleton during operation and also allows for some adjustability on the wearer. The shank component consists of a hex-shaped rotational bar, pulley on which the Bowden cable is terminated and aluminum bar extending from the knee to ankle. The human interface is connected to the wearer by four straps at the ankle, upper calf, lower thigh and upper thigh. In order to maximize leverage about the knee and minimize magnitude of forces applied to the wearer for a given torque, straps were located as far from each other as possible for their respective components (i.e. calf distance from ankle and upper thigh from lower thigh). Figure 4.1 shows exoskeleton composition.

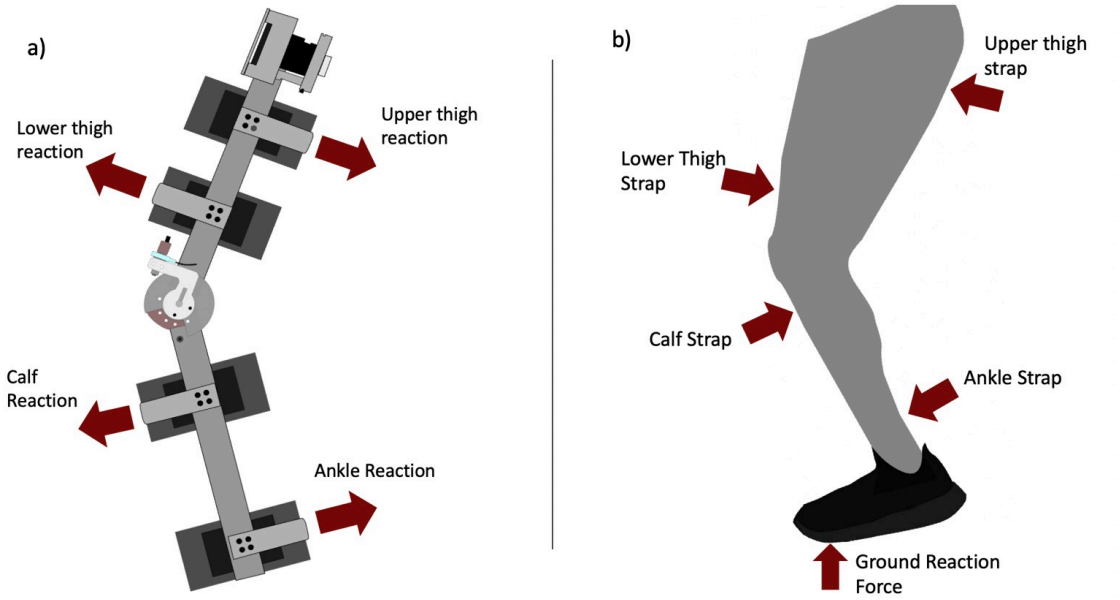

Figure 4.11: a) shows the reactionary forces on the exoskeleton as worn b) shows the corresponding forces on the leg from exoskeleton to produce an assistive torque at the knee joint

Free body diagrams (FBD) as shown in figure 4.11 were analyzed assuming that the axis of exoskeleton joint rotation is approximately aligned with the axis of knee joint rotation and that forces act normal to the thigh and shank of the wearer. FBDs show the net force placed on the leg of the wearer and the reactionary forces placed on both components of the

human interface. In addition to forces presented, small shear forces are expected to occur at the straps but are difficult to quantify, as a result the forces analyzed are assumed to be an approximate representation.

4.4 Electronics and Control

4.4.1 Hardware

In order to properly replicate motion profiles and determine accurate actuation output for providing assistance to an individual, a system of sensors and microcontroller unit (MCU) must be implemented for feedback and computation. As determined through literature review and system requirements, the most important variables to be measured are joint angle, torque and velocity. Measurement of joint angle and velocity are collected through magnetic incremental encoders (RLS magnetic encoders), figure 4.12, located at the motor and exoskeleton knee joint. The encoder is a two component device with a rotating magnetic actuator and encoder readhead. As the magnetic actuator rotates the readhead senses changes in the magnetic field and converts that information to rotational data. The encoder loacated at the motor is used to provide feedback in the Instaspin motion control at the motor level, which dictates motor performance. The knee encoder is placed at the rotation of the knee joint with the magnetic actuator press fitted into the rotational shaft of the exoskeleton. The knee encoder detects angle of exoskeleton knee joint and provides angular input for calculation of the desired torque assistance based on an angle-based torque control scheme. The joint torque is calculated by first collecting force data in the cable tension with a single-axis donut load cell (Futek LTH300), figure 4.13. The load cell is positioned in line with the Bowden cable at its termination point as shown in figure 4.14. Using the acquired cable

forces and known structure geometry, joint torque can then be calculated with the equation below.

$$\tau_{knee} = F_{cable} * r_{pulley} \tag{4.4}$$

Here, τ_{knee} is the torque at the exoskeleton knee joint, F_{cable} is the force measured by the load cell and r_{pulley} is the radius of the pulley located at the knee. In addition to the current sensors, future work may install inertial measurement units (IMUs), force switches or electromyography (EMG) sensors to detect user intention and improve human-exo interaction.

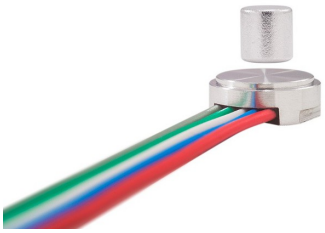

Figure 4.12: Super-small non-contact incremental rotary encoder (RLS)

Figure 4.13: 250 lb LTH 300 Futek donut load cell

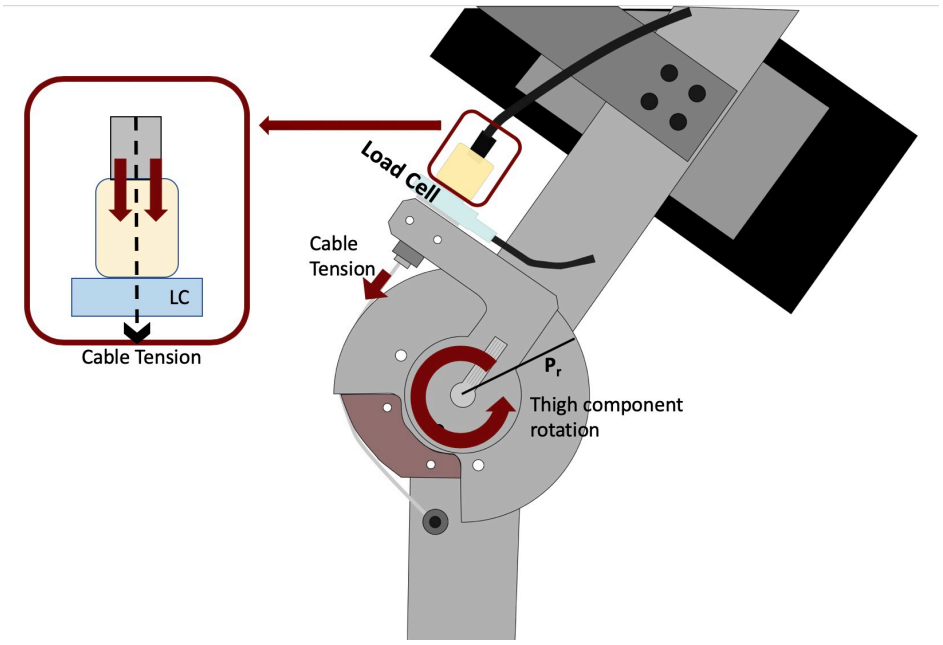

Figure 4.14: placement of load cell in order to measure forces in the cable as extension occurs

A single C2000 Texas Instrument MCU (F28069M) is used to read sensor output, determine correct response, control actuation and data log through serial communication to graph and analyze the exoskeleton motion profile. The MCU is outfitted with a motor controller shield (TI DRV8305EVM) which drives the BLDC quadcopter motor, instrumentation breakout board for sensor integration and an amplifier for load cell operation. MCU and board setup is shown in figure 4.15. Current limitations of the system are created by the motor controller shield as it has a max current of 20 A. The shield was chosen for its compatibility with TI's Instaspin motion and is still capable of satisfying design requirements.

The system is powered by a 6s LiPo battery producing 22.2 V. The supplied power is connected to both the motor controller shield and instrumentation breakout board. The motor controller shield drops the voltage to 3.3 V to power the MCU and incremental encoders. The instrumentation board uses a voltage regulator to drop the input voltage to 12 V so that the power supply is within the usable excitation voltage range of the load cell. The 12

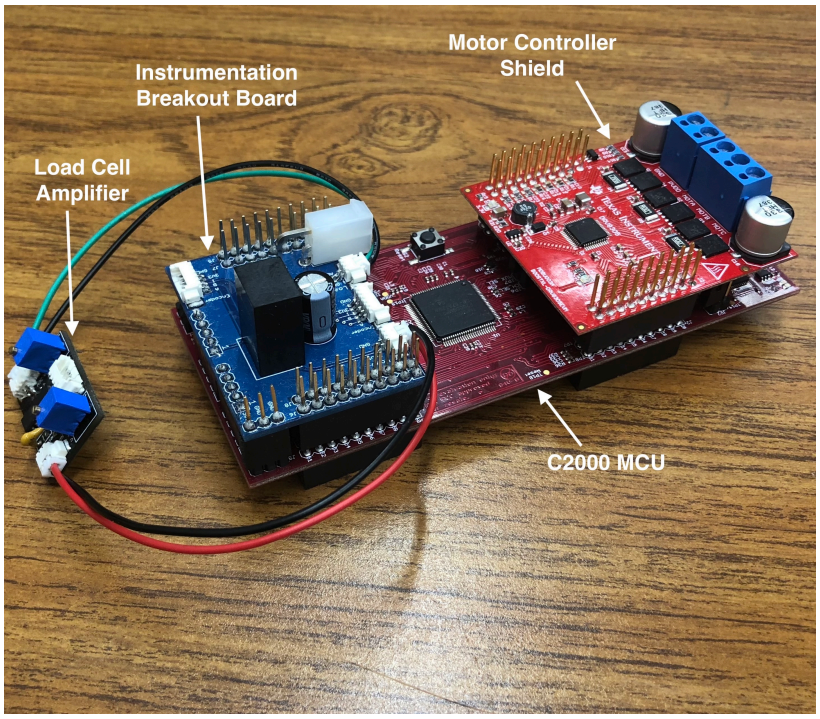

Figure 4.15: MCU, Motor Controller shield, Instrumentation breakout board and Load Cell amplifier board setup

V line is then passed from the instrumentation board to an amplifier that is connected to the load cell. Figure 4.16 provides an electrical system block diagram. Figure 4.17 presents an Eagle CAD board schematic for the instrumentation breakout board.

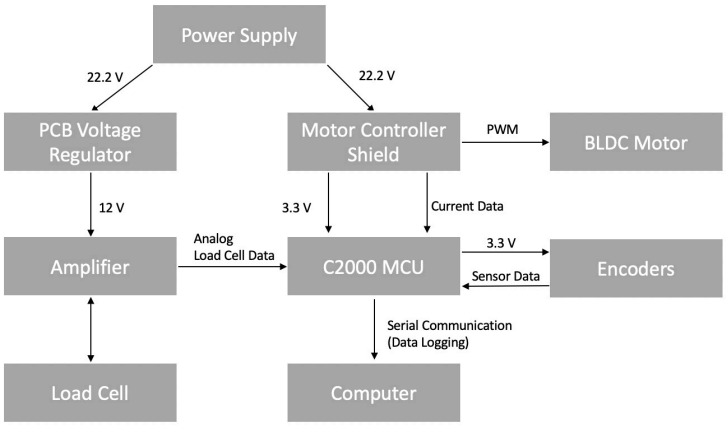

Figure 4.16: Electrical system block diagram

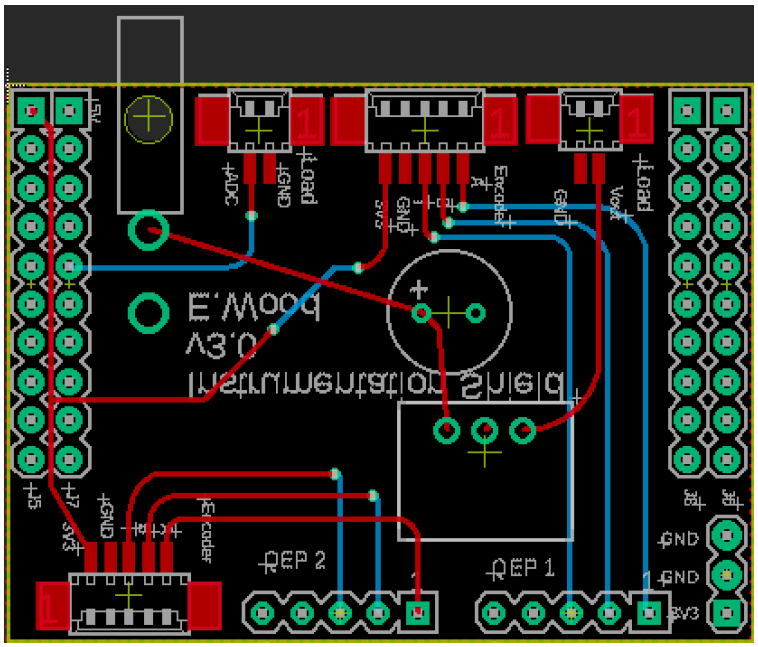

Figure 4.17: Instrumentation Breakout Board Eagle CAD board schematic

4.4.2 Control System

Many active exoskeletons can be separated into a few subsystems that compose the overall device; one such system is the control system. The control system is vital to correct operation of assistive wearable devices as it takes in information and determines the correct responses based on a desired goal. In an effort to lay the foundation for a future more complex control system, the exoskeleton described in this thesis aimed to implement an angle-based torque controller. This type of controller builds off the angle-torque relationship found in literature to apply varying amounts of assistance based on the degree of knee flexion. Using this control strategy it is possible to assist in both lifting and STS tasks in a time independent manner throughout their motion.

The angle-torque control system designed here uses reference data and a knee joint encoder to develop a feedforward control that assist the wearer during STS. In order to develop this system, angle and torque data acquired from literature were plotted and equations were

developed to approximate features of the curve. The angle-torque curve needed to be broken down into three sections, 10-81°, 81-92.5° and 92.5-105° as shown in figure 4.18. Figure 4.19 shows the resulting current command curve that is sent to the motor controller. The curve possesses a similar shape to that of the angle-torque curve as expected due to current and torque being linearly related by a torque constant.

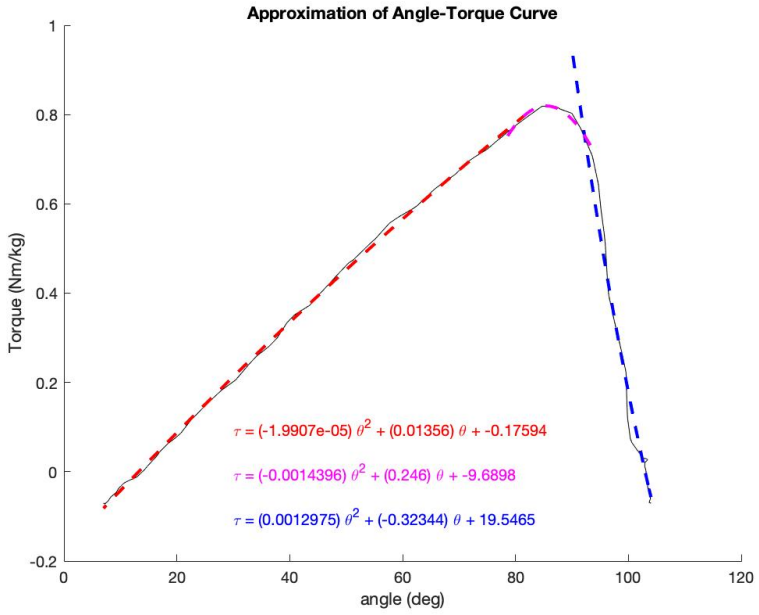

Figure 4.18: Approximation method of angle-torque data from literature review using three curves

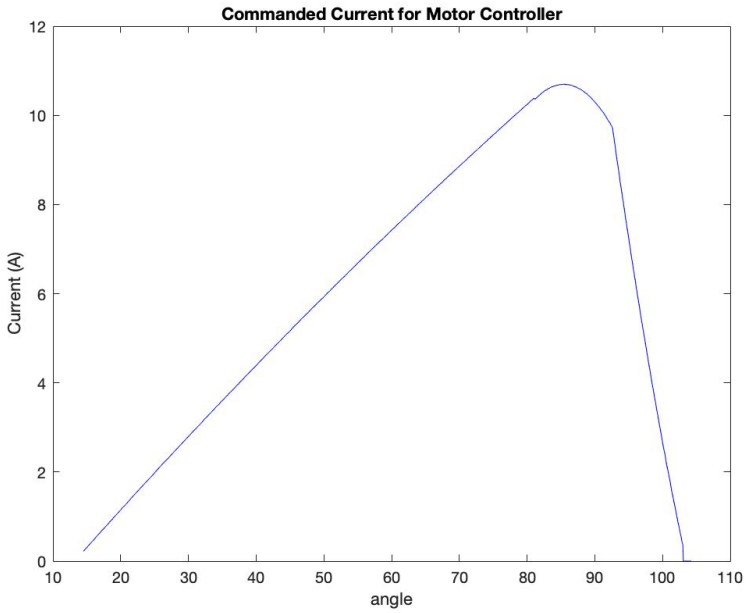

Figure 4.19: Current command profile calculated from angle-torque curve approximation. Directs motor output at specified angles

Once motion has begun, the encoder located at the knee determines joint angle and sends the information to the MCU. The MCU uses the appropriate equation based on current knee angle to calculate the desired level of torque. This level of torque, correlates to a corresponding current using equation 4.3. The MCU then commands a specific current input and resulting torque output of the motor that is multiplied by the gear and pulley ratios to produce the desired torque at the knee joint. Figure 4.20 shows an overall block diagram of the angle-based torque controller. This controller was chosen as it provides flexibility in timing, can consistently contribute a specific amount of mechanical work towards motion and will not amplify the errors already present in poorly controlled knee torques of less able-bodied individuals that can occur during STS. In the future the load cell will be incorporated to measure force in the cable which can then be used to calculate the torque delivered to knee. The measured torque can then be sent back to the controller to calculate a more accurate desired output.

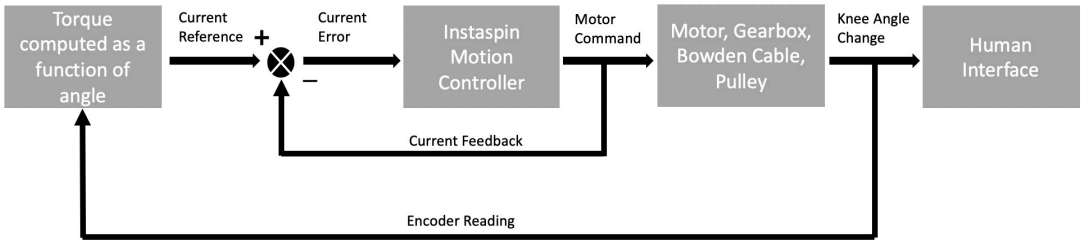

Figure 4.20: Block diagram of angle-based torque control for STS assistance

4.4.3 Data Logging

Data logging is important for analysis and evaluation of exoskeleton performance. The MCU will log joint angle, motor angle, joint velocity, load cell force and motor current through serial communication. Each value package is composed of a beginning identifier, a start and stop bit with no parity and two bytes of actual data. In order to log data over serial communication two factors had to be solved, communication speed and data packaging manipulation. Speed was calculated based on a data package composition of a maximum of 25 bytes sent per cycle, with a sampling rate of 100 HZ thus resulting in a required communication speed of,

$$Comm_{speed} = 10 * 25 * 100 = 25,000bps \tag{4.5}$$

Therefore, to allow for extra time for the MCU to perform other necessary tasks and satisfy the data logging requirements a standard speed of 115,200 bps is chosen.

Data packaging manipulation is necessary because UART serial communication is only capable of sending 8-bit data packages at one time. The data being logged is a 16-bit value so the value must be split into a most significant bit (MSB) and least significant bit (LSB) using bit shifting. Once the value is separated, the identifier is sent to the computer telling

it which data type to expect, then the MSB and lastly LSB. Once the computer receives all three parts of information, an external software called processing recombines the MSB and LSB and stores the value in a data table. Post-processing of logged data is done through a Matlab script allowing easier graphing and analysis of exoskeleton performance.

4.5 Finite Element Analysis

As part of the design process, finite element analysis (FEA) is performed to verify all exoskeleton components' structural integrity under expected heavy loads and impacts. The factor of safety for several key components are shown in figure 4.21. Components include the Bowden cable sheath termination point at the actuator, gearbox output shaft, output pulley and support posts for the sheath termination at the knee. These components were chosen because their failure would be attributed to excessive forces beyond those designed for, and render the exoskeleton useless. Material for all parts in the exoskeleton are aluminum-6061 with the exception of the gearbox shaft, output pulley and Bowden cable sheath termination post, which are aluminum-7075 T6.

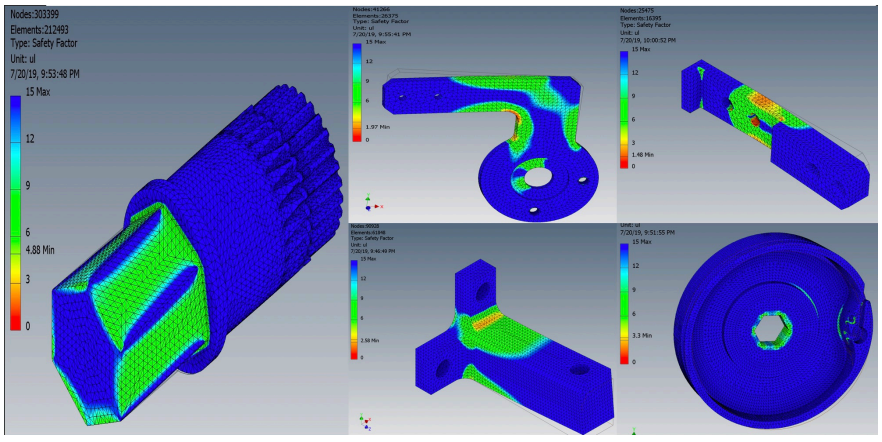

Figure 4.21: Left: Hexagonal output shaft, Middle Top: Outside connector of human-interface, Top Right: Output Pulley, Middle Bottom: Cable sheath termination post at the actuator, Bottom Right: Inside connector of Bowden cable termination support

Chapter 5

Preliminary Evaluation

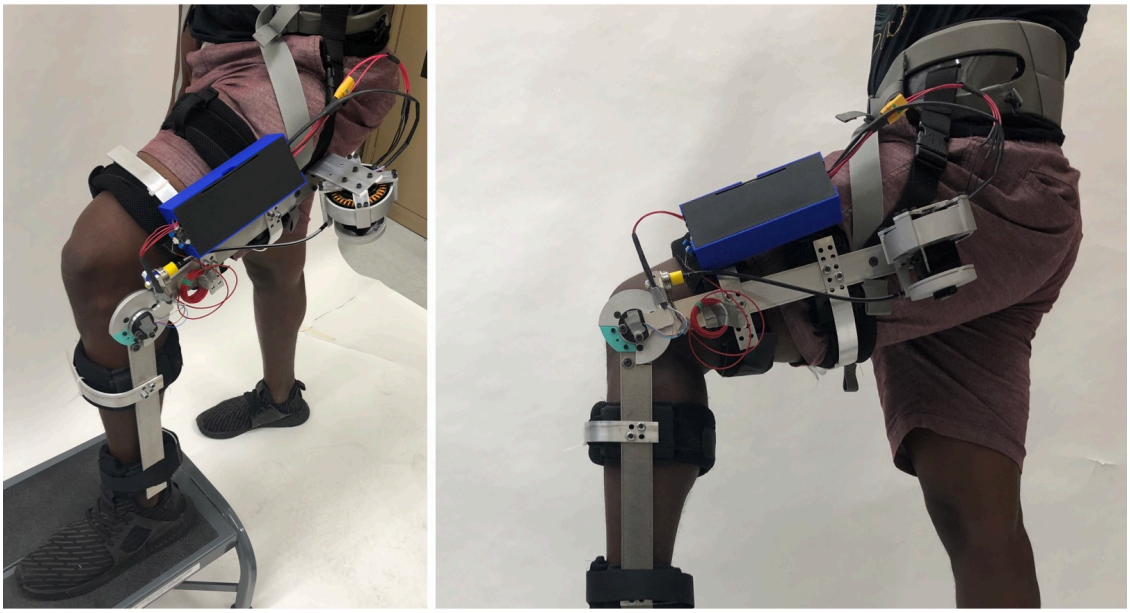

Figure 5.1: Active knee exoskeleton on wearer

The fully prototyped knee exoskeleton extends from about the hip to ankle of a 6' tall wearer and weighs 2.5 kg, with the actuator accounting for 0.9 kg. It has a range of motion from -5 to 115°. The padded straps are composed of soft foam and wrapped in a mesh fabric. While worn the exoskeleton has limited axial and torsional movement about the leg due to the support of the waist belt and strapping. The largest lateral protrusion is created by the actuator unit and is approximately six inches from the leg. While the actuator is backdrivable, evaluation of the actuator unit shows that friction of the motor and gearbox combination is more then expected, making it not as backdrivable as initially desired. Initial

evaluation of exoskeleton operation focused on motor ability to perform according to desired angle-based torque control schemes. For these initial test, current was scaled-down by a factor of ten (max value of 1.1 Amps) and the human interface component was manually rotated through it's range of motion while the motor's generated torque was recorded and evaluated. This test was ran with just the motor and then ran with the full actuator. After these test, the actuator was connected to the knee by bowden cable and allowed to autonomously simulate STS motion while knee angle, motor current and torque were recorded. The results for testing are presented below and show the behavior of the motor as compared to the desired output.

5.1 Motor Testing

The first test of motor testing is conducted with the motor unattached to gearbox. The human interface is manually moved in an attempt to execute a similar motion profile to that of STS, in which the knee begins at a heavily flexed angle (approximately 100°) and moves to fully extended. Figure 5.2 shows the motion profile that was recorded using the encoder at the knee. It is to be noted that this simulated motion occurs over a longer period of time then the average STS motion.

Figure 5.3 shows the commanded current profile versus angle in the top graph and the measured motor current in the bottom. Figure 5.4 presents the torque curves for both commanded and calculated torque versus time. Torque was calculated by $\tau = I_a * K_t$. Observation of both figures shows that the measured current and calculated torque, while volatile, follow the trend of the desired angle-torque curves.

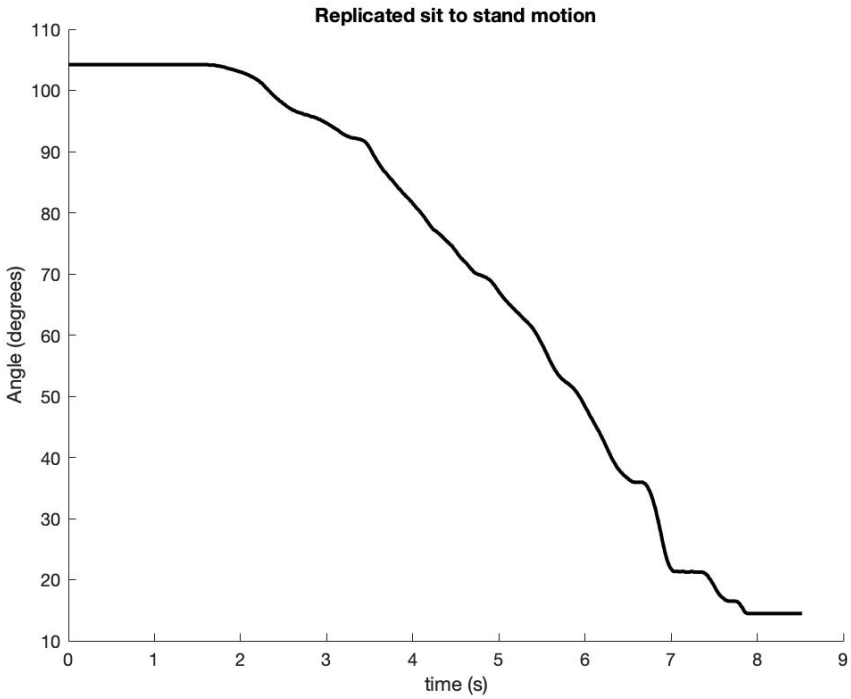

Figure 5.2: Simulated motion of Sit to Stand used to observe motor performance according to angle-based torque controller

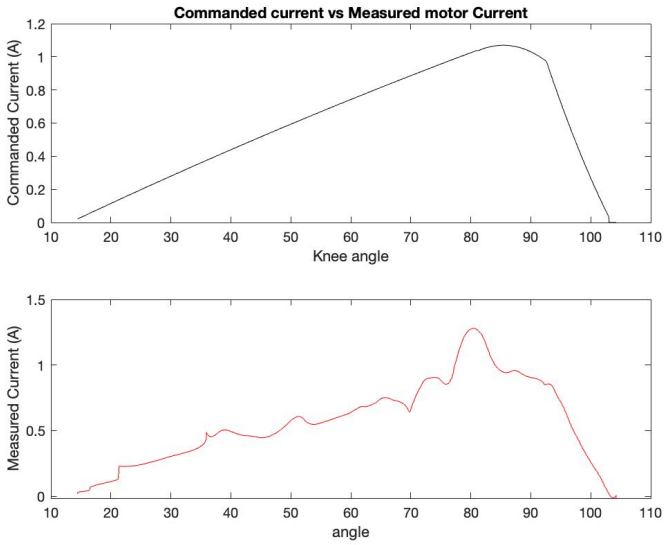

Figure 5.3: Commanded current generated by approximation of angle vs torque curve compared to the measured motor current during testing

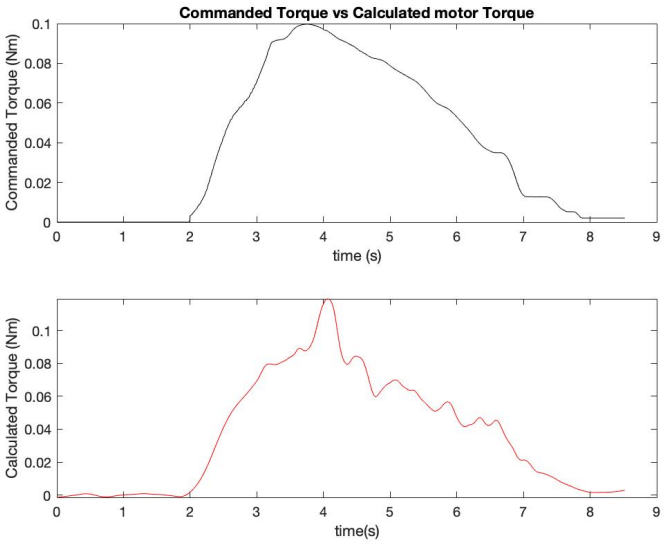

Figure 5.4: Commanded torque vs time compared to the calculated motor torque vs time during initial testing

The second test of motor testing had a random motion pattern in which the knee human interface was extended and flexed at varying speeds to observe the motor's ability to track and execute the control scheme. Figure 5.5 shows the motion profile that was executed during testing. Figure 5.6 show the commanded current versus angle profile compared to its measured counterpart. Figure 5.7 shows the commanded torque versus time compared to the calculated torque versus time.

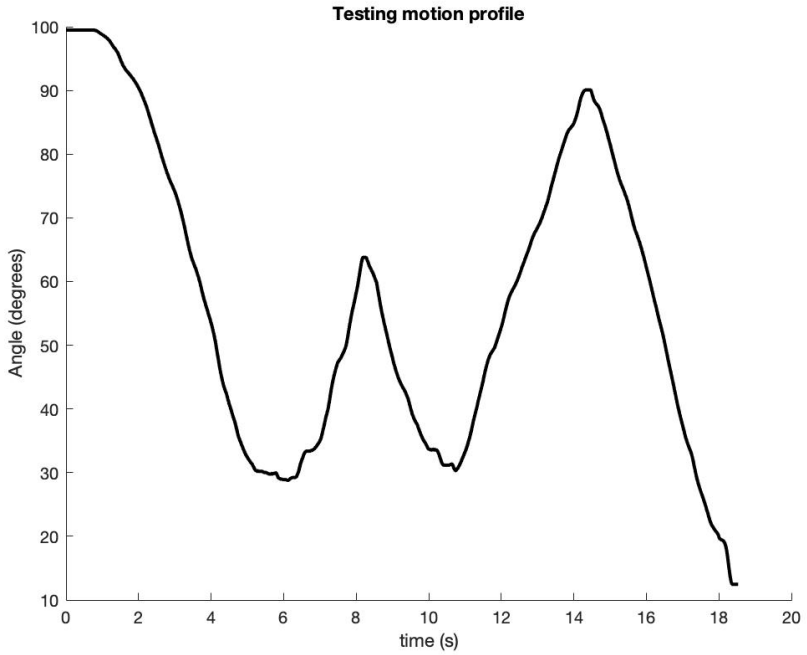

Figure 5.5: Random motion profile of knee exoskeleton during testing of motor's angle-based torque execution

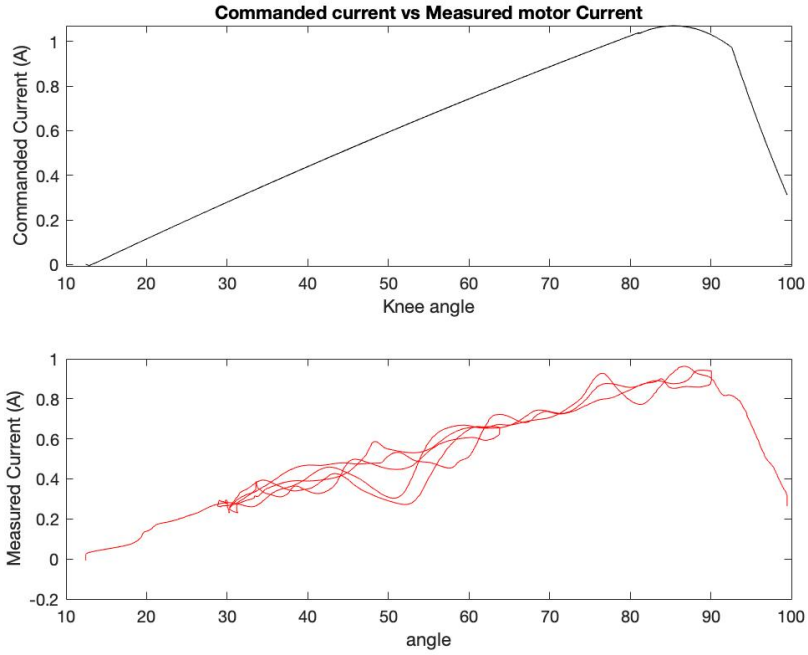

Figure 5.6: Commanded current compared to the measured motor current during random motion of the knee

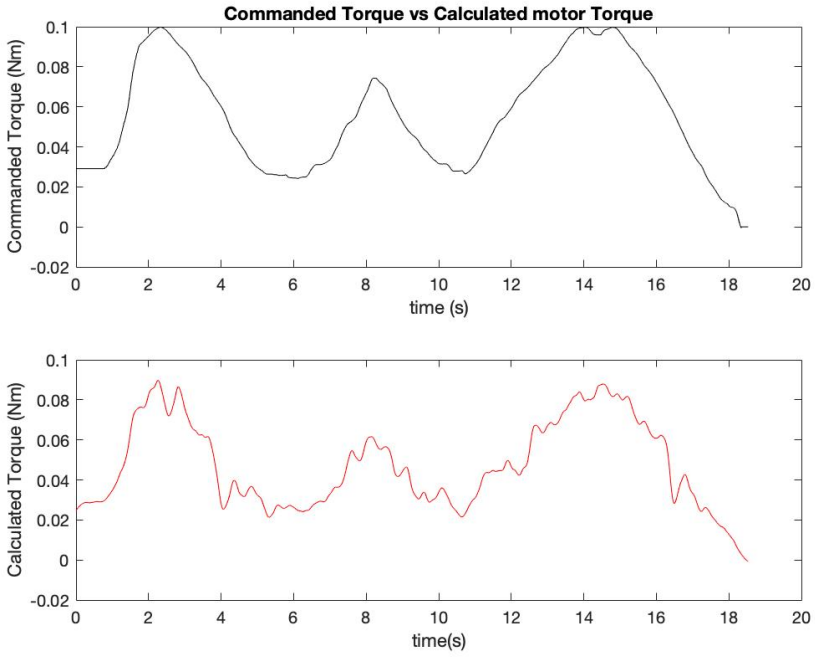

Figure 5.7: Commanded torque vs time during random motion testing as compared to the calculated torque vs time

5.2 Actuator Testing

The second section of testing was conducted with the motor paired to gearbox and pulley but unattached to the human interface. Testing for the motor and gearbox pairing followed a similar pattern to that of the previous testing of the single motor. Current was scaled-down by a factor of 10 and the actuator's ability to perform along commanded angle-based torque scheme for a motion similar to STS and random was evaluated. The first test was a simulated STS and results are presented below.

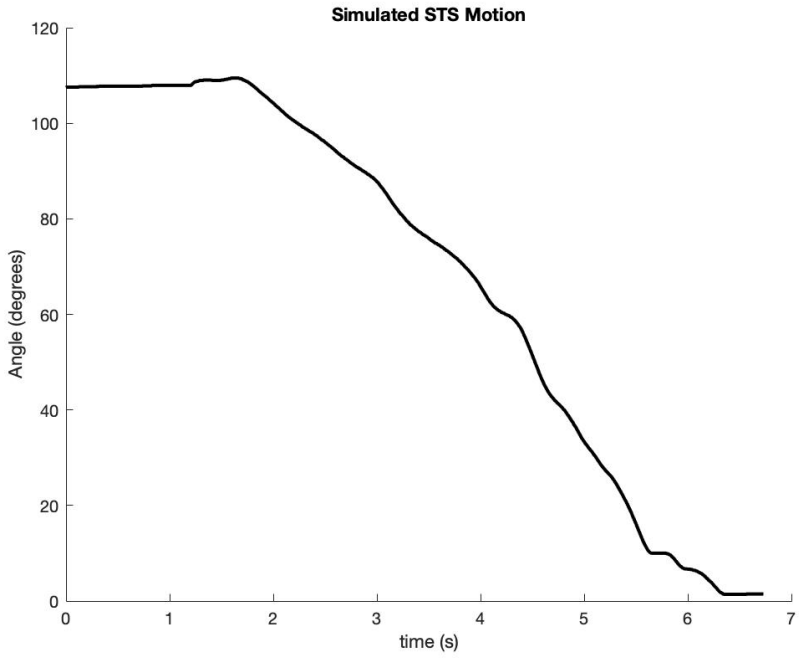

Figure 5.8: Simulated STS motion profile of knee exoskeleton during testing of motor and gearbox's angle-based torque execution

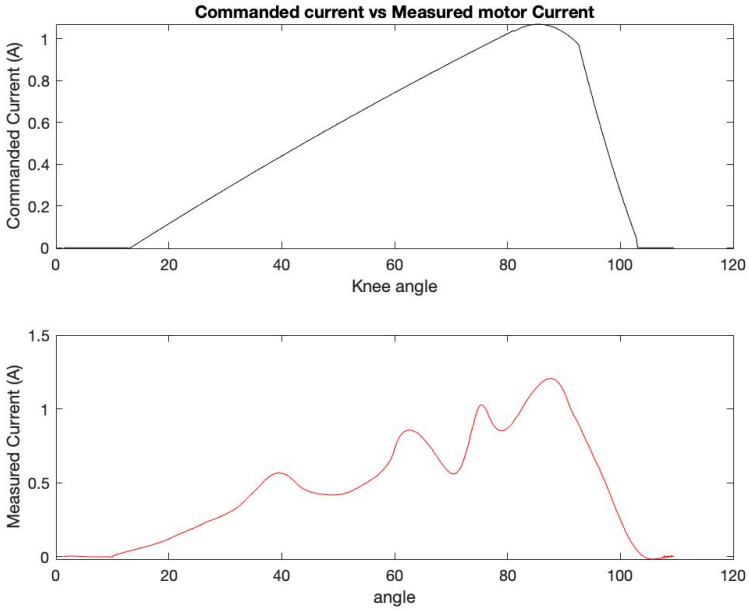

Figure 5.9: Commanded current generated by approximation of angle vs torque curve compared to the measured motor with gearbox current during simulated STS motion of the knee exoskeleton

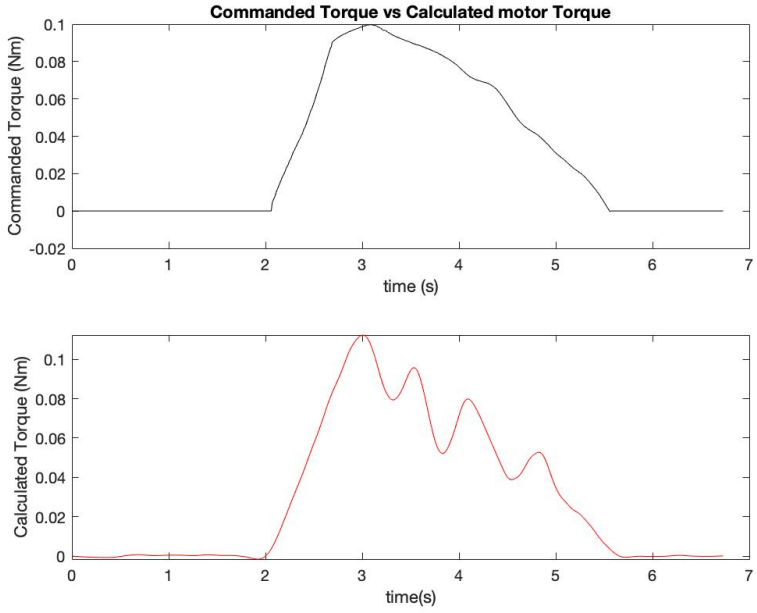

Figure 5.10: Commanded torque vs time compared to motor with gearbox calculated torque vs time during STS motion testing

Random motion began from a heavily flexed angle reached 60 degrees and quickly reversed directions. Once the exoskeleton joint reached the start point, it was reversed again and continued until full extension. Actuator results for random motion are presented in the following figures.

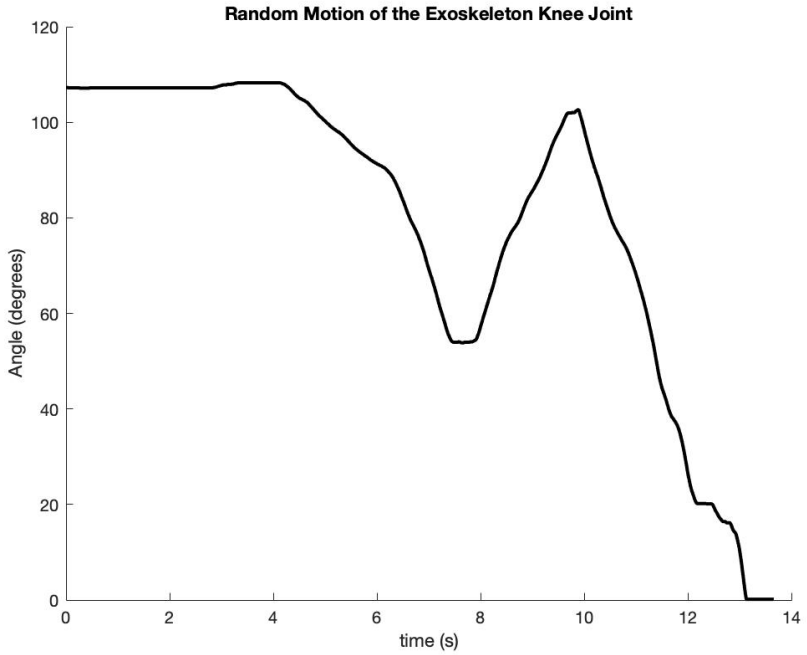

Figure 5.11: Random motion profile of knee exoskeleton during testing of motor and gearbox's angle-based torque execution

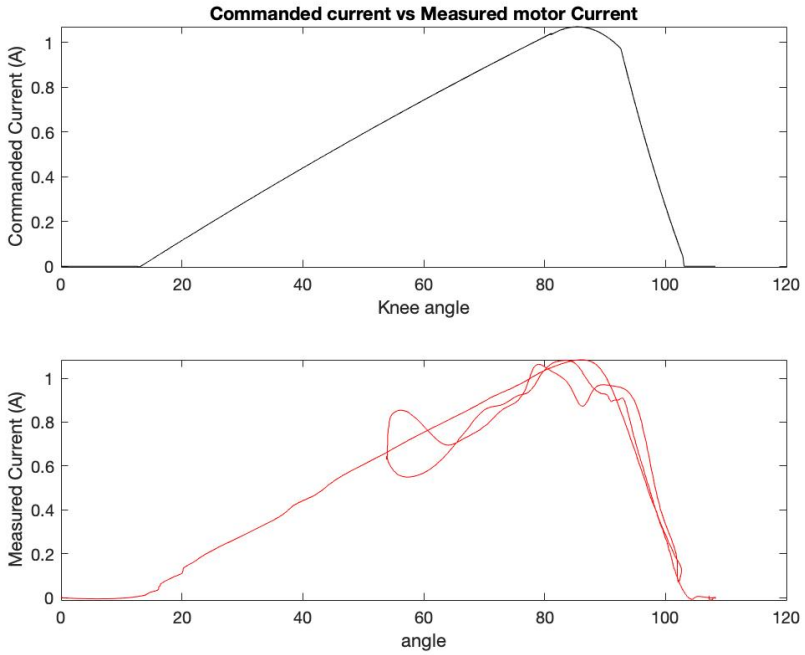

Figure 5.12: Commanded current compared to the measured motor with gearbox current during random motion of the knee exoskeleton

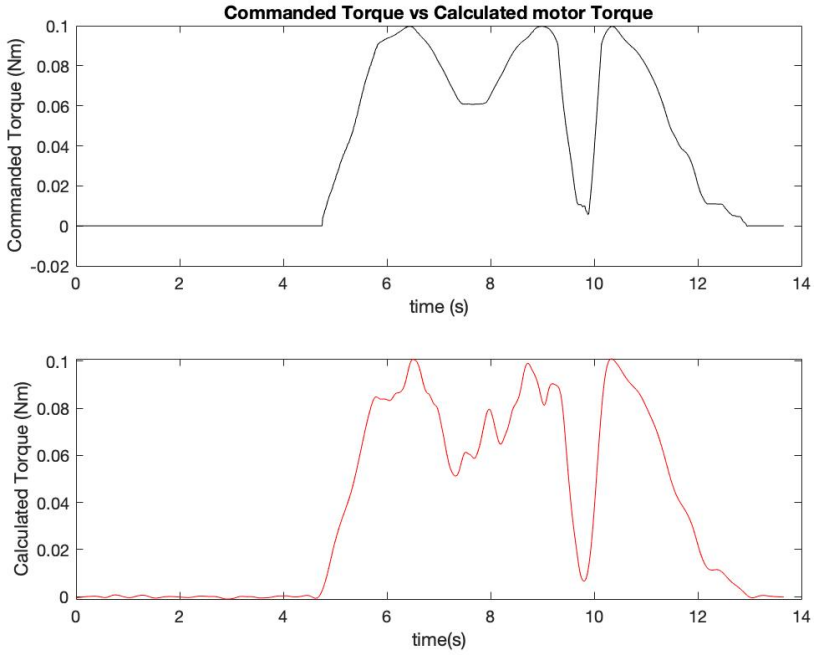

Figure 5.13: Commanded torque vs time compared calculated torque vs time during random motion testing for motor and gearbox pairing

5.3 Full Exoskeleton Test

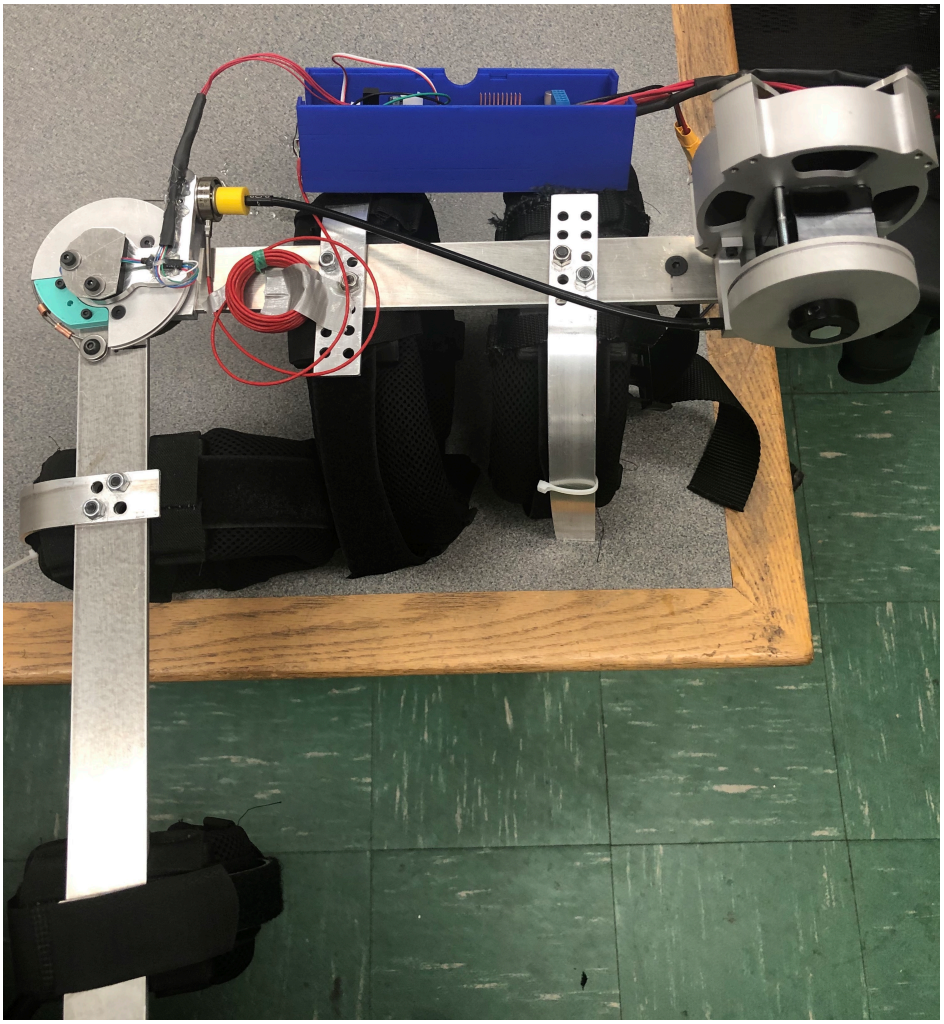

Figure 5.14: Fully assembled Exoskeleton for autonomous motion testing based on angle-torque scheme

Next testing involved full setup of the active knee exoskeleton (figure 5.14) to allow for autonomous motion through the STS profile. During this testing current had to be increased from previous test as the torque produced was not enough to move the human interface through the full motion profile. Current is still scaled down by a factor of 3.75 from the application current of 11 Amps that is used when being worn for STS. The test was performed by starting the exoskeleton at a heavily flexed angle, then moving the exoskeleton to a

start angle of 104 degrees in which the angle-based torque scheme takes effect. Once the exoskeleton begins moving a slight external resistance is manually applied to slow movement and evaluate exoskeleton performance against resistance as it would have when being worn. Motor current and torque data were collected in similar manners as previous test, joint angle was collected by the incremental encoder at the knee and knee torque was calculated by using load cell force readings and known structural geometry. Results of this test are presented below.

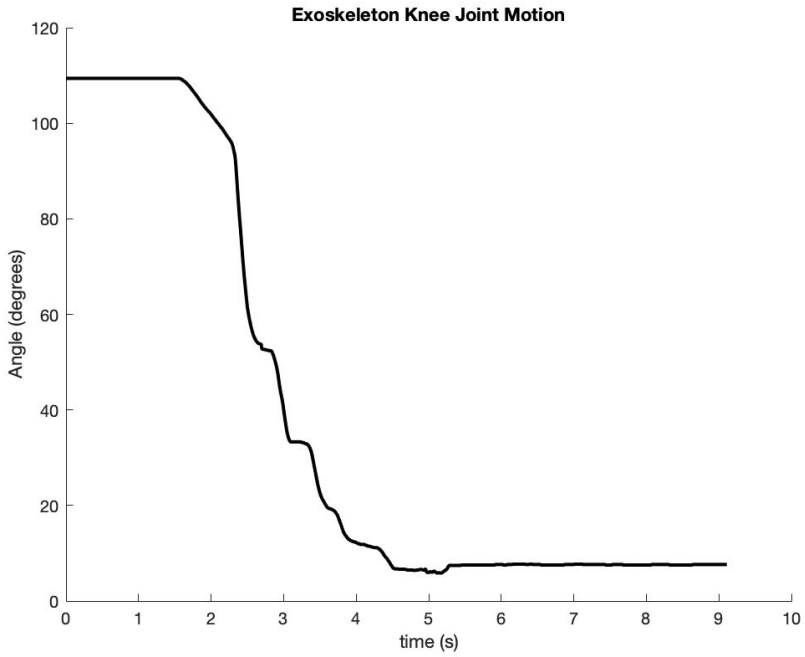

Figure 5.15: Simulated STS motion profile of knee exoskeleton as actuated by the distal actuator based on angle-based torque control

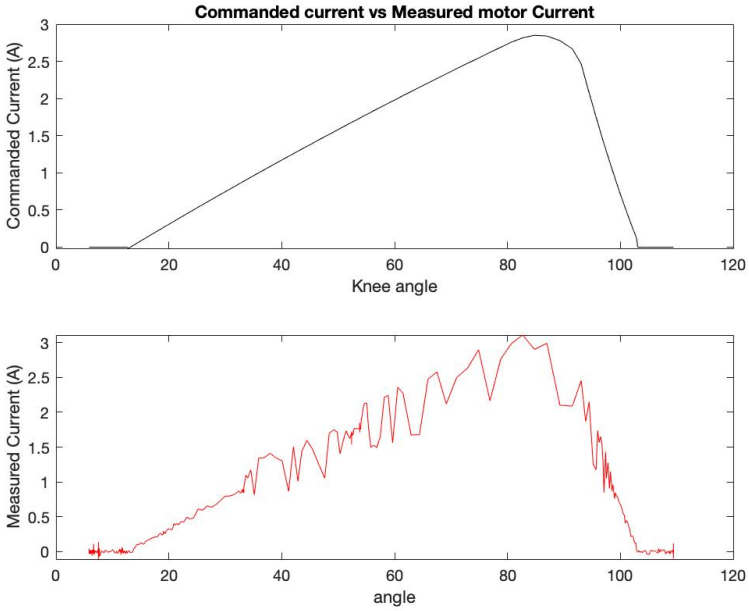

Figure 5.16: Commanded current compared to the measured current during actuated motion of the knee exoskeleton

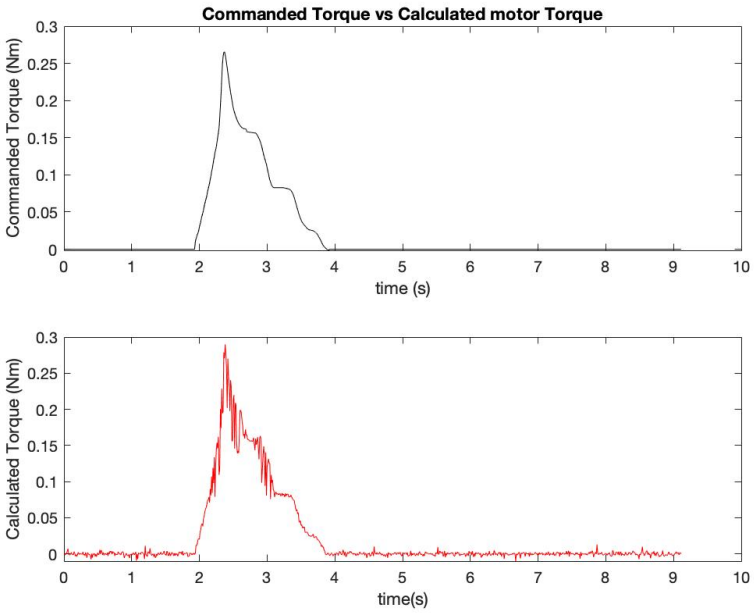

Figure 5.17: Commanded torque vs time compared to motor calculated torque vs time during actuated motion testing

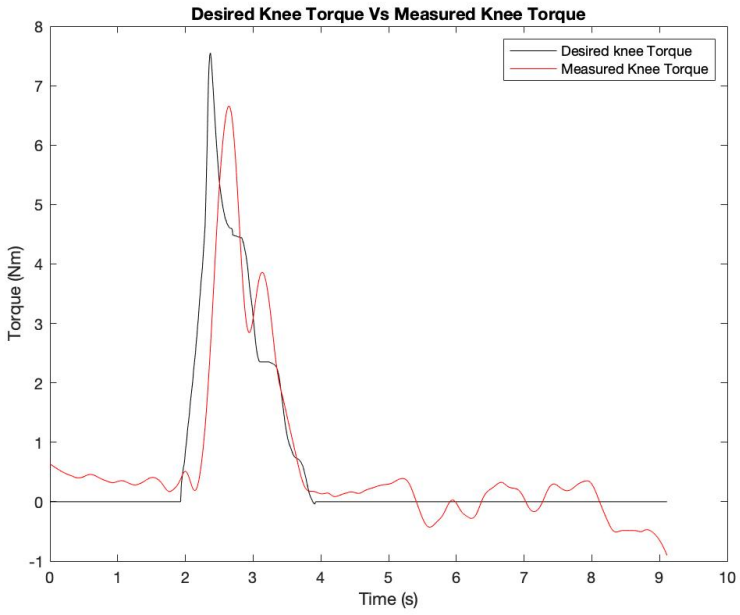

Figure 5.18: Desired knee torque compared to the knee torque calculated by load cell force measurements and structure geometry during actuated motion testing

Results of fully actuated knee exoskeleton testing shows that the motor is capable of performing as desired under device loads and additional external resistance. Measured motor current and calculated motor torque followed the trend of goal performance. Knee torque showed trend similarities between desired and measured. Measured torque reached a joint torque of 6.65 Nm, resulting in a maximum torque output less than that of the peak of 7.55 Nm that was shown in desired knee torque. Efficiency factors such as torque losses in the gearbox and friction in the bowden cable are the most likely causes for differences between desired and measured torque.

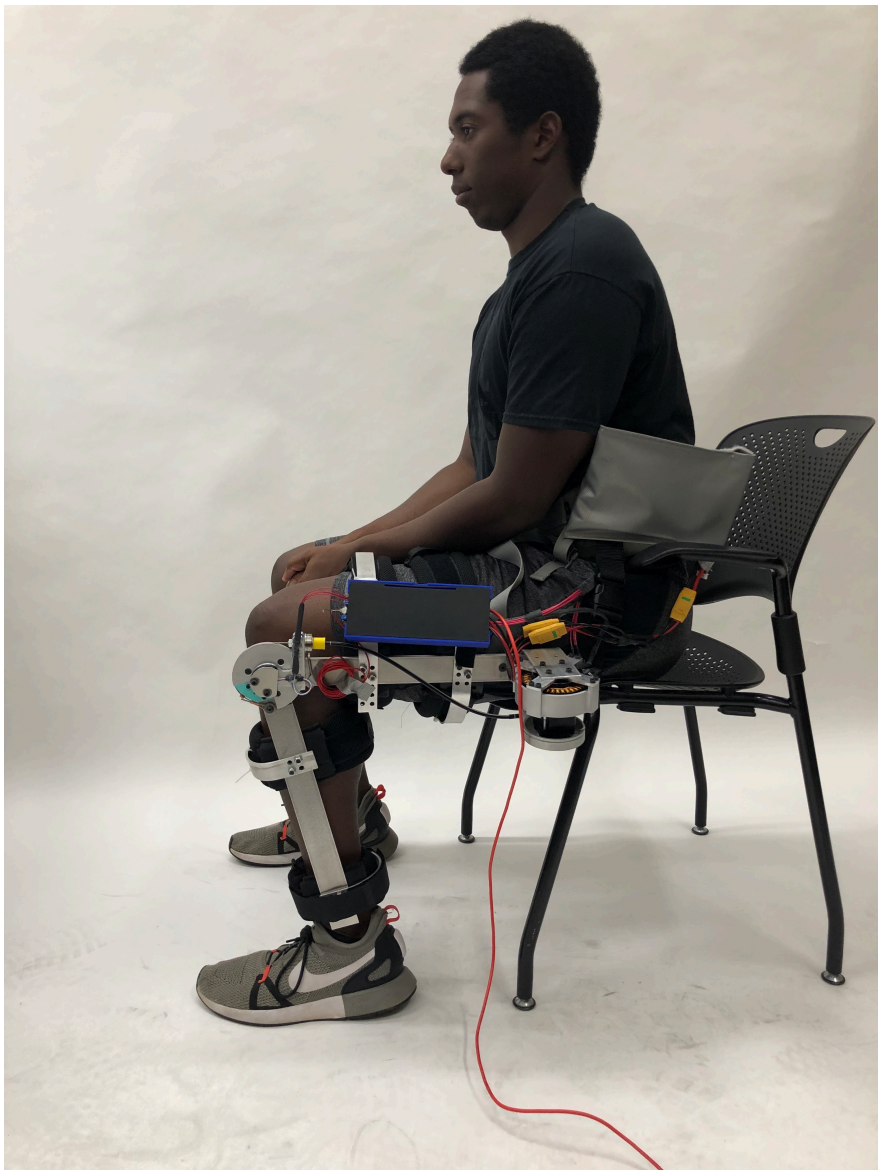

Figure 5.19: Active knee exoskeleton being worn for STS motion testing

Lastly, the exoskeleton was put on an individual and then STS was performed. During this test the exoskeleton was allowed to actuate at full current and the corresponding torques to apply assistance. Results are shown below.

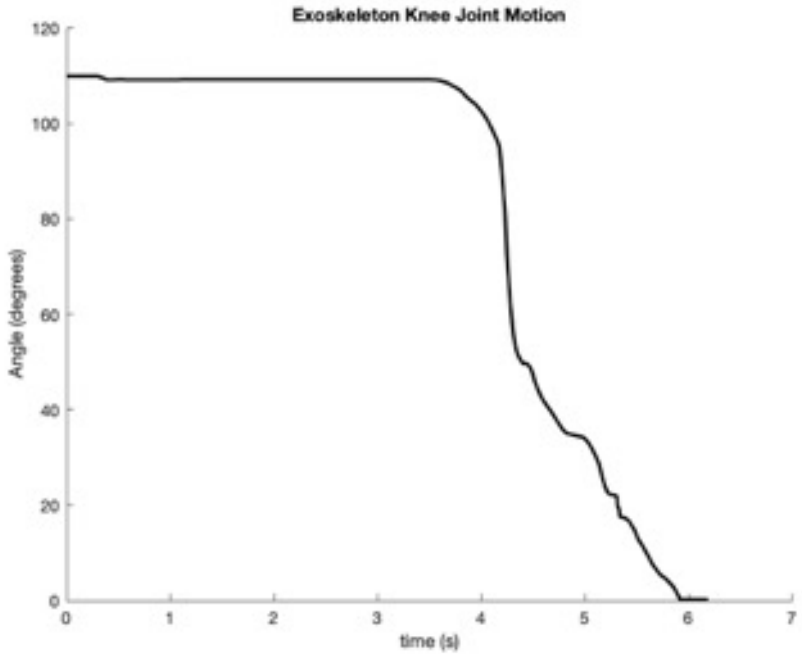

Figure 5.20: Motion profile of knee exoskeleton during STS motion on user

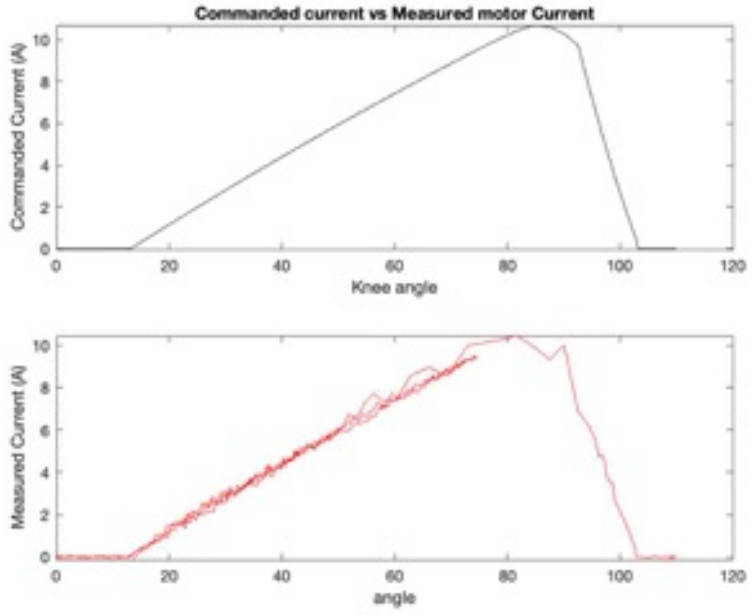

Figure 5.21: Commanded current compared to the measured current during STS motion testing

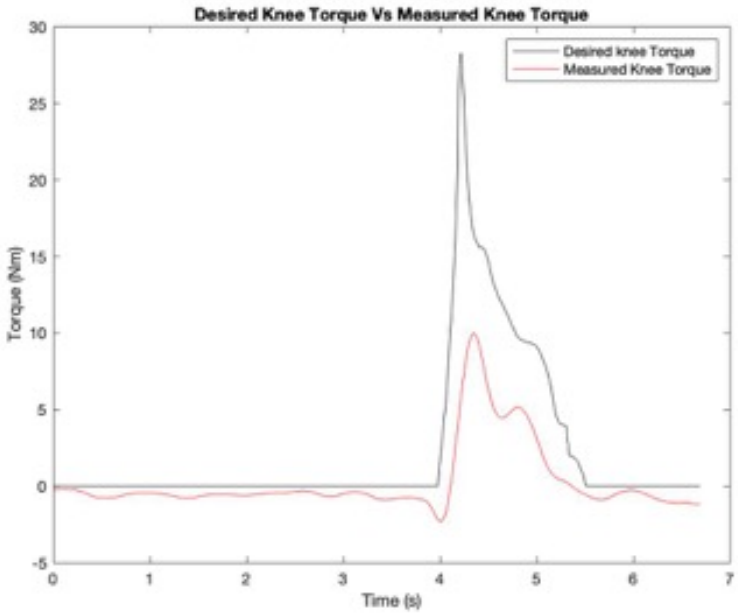

Figure 5.22: Desired knee torque compared to the knee torque calculated by load cell force measurements and structure geometry STS on user

Results of testing on wearer show that the motor is capable of performing according to desired torque control and that the exoskeleton can provide assistance when expected. Torque data shows that the exoskeleton is able to provide some level of assistance although it is not nearly as much as desired. It is believed that the lack of torque produced at knee joint is due to higher forces in the exoskeleton causing higher friction within the gearbox and cable pathway thus creating greater efficiency loss.

Chapter 6

Conclusions and Future Work

The exoskeleton presented in this thesis is designed and prototyped to be an active, one DOF knee exoskeleton capable of providing assistive extension torques for farmers performing ADL. The ADL designed for include sit to stand, hill navigation and stair navigation. These tasks can require up to two to three times the biomechanical joint torque needed in walking, which can prove to be difficult for elderly farmers to achieve due to muscle weakness or age-related diseases. In order to assist these farmers and prevent further injury this exoskeleton was designed to provide up to 30% of knee torque required for ADL. Assistive torques are generated by a distally placed BLDC motor and gearbox combination that uses bowden cable and pulleys to transfer torques to the exoskeleton knee joint. Forces are then applied to the wearer through four leg straps located at the upper thigh, lower thigh, calf and ankle. Implemented in this exoskeleton is an angle-based torque controller that determines the level of assistance to be applied based on the degree of knee flexion. By using this controller, the exoskeleton is able to consistently apply mechanical work to movement and is less dependent on the time profile of motion to assist wearers. In preliminary evaluation of the knee exoskeleton design, weight, comfortability and control scheme execution were evaluated. In all of these areas the exoskeleton shows promise and is capable of executing an angle-based torque scheme in scaled-down current testing, but further developments and improvements must be made to reach the ultimate goal of helping farmers. Overall, the exoskeleton presented is an initial prototype that lays the framework for further design and

control improvements that will help create an active knee exoskeleton capable of taking some of the load off of farmers as they perform their ADL.

6.1 Future Work

The exoskeleton described in this work lays the foundation for producing an active wearable device that is capable of assisting farmers in their everyday activities. However, several improvements must be made in order to fully reach that goal, such as further development of an assistance as needed strategy, gait phase and action recognition, and control system and design improvements. This section provides a brief overview of future work that should be performed in order to begin field testing with farmers.

6.1.1 Improvements

As discussed previously, goals of this exoskeleton include lightweight, low profile and comfortability. As it is currently all three of these areas can be improved upon. In order to fix the current design flaws several changes can be made. The first change is to perform more stress analysis and possibly remove excess material in the human interface frame. The bars are relatively heavy and have a large safety factor; by systematically redesigning them to have less material the exoskeleton will lose a lot of mass, while also being capable of handling expected forces. This will be easier on the wearer and increase comfortability as the exoskeleton won't tend to slide down against the support of the waist belt. Another change that can be made is to the leg straps. The straps can be improved by stitching the velcro to the actual padding of the strap. Currently, when worn the velcro straps that secure the exoskeleton to the wearer tend to slide off of the pad making it uncomfortable to wear for

long periods of time and necessitates adjustment.

In order to decrease volume size of the exoskeleton the actuator must be placed even closer to the exoskeleton. This is done by switching the Bowden cable sheath termination post to the other side of the motor frame and also flipping the Bowden cable secure point on the output pulley. Completing this flip will allow the actuator to be secured flush to the upper thigh strut of the exoskeleton without introducing too much friction in the Bowden cable pathway.

Another area of improvement is backdrivability. The first suggestion is the incorporation of an elastic element between cable termination and pulley at the knee. An elastic element will allow for some initial range of movement and grant time for the actuation unit to respond to unexpected perturbations. The harmonic drive FLA rotary actuator can also be evaluated as a substitute to the current designed actuator as it has the gearbox and motor in one package and greatly reduces the height of the actuation unit. The FLA rotary actuator substitute will help to solve the backdrivability issues (discovered after assembly of the actuator) due to high friction within the two stage gearbox and motor, by replacing it with a harmonic drive. It is suggested that a gear ratio less than 60 in harmonic drives allows for backdrivable actuators [51].

A possible addition to the exoskeleton that can improve overall operation is the inclusion of a limit switch for zeroing encoder angle. Currently, the exoskeleton uses an incremental encoder at the knee to detect flexion angle, which is calibrated manually by resetting count when the wearer's leg is fully extended. In order to automate this process, inclusion of a limit switch at a known position will allow the wearer to hit this switch and calibrate the encoder accordingly.

6.1.2 Electronics: Controls

The current control implemented in this exoskeleton can be further developed to improve overall performance. The first improvement is taking into account the mass and torque required to actuate the exoskeleton and adding it to our expected biomechanical torques, allowing all of the intended torque to be delivered purely to assistance. The second improvement is developing the current controller into a feedback controller that makes decisions based on the error between desired torque and the measured torque delivered to the knee. Creating a feedback controller is essential in developing an exoskeleton that is useful in a farming environment. It takes into account the error between exoskeleton output behavior and desired behavior to determine the best course of action to deliver assistance. Below, an example controller is outlined and a block diagram that will be simple to implement based on current exoskeleton components is presented (figure 6.2).

The angle-torque control system designed here uses the Texas Instrument (TI) Instaspin motion as a foundation, strips away some of the additional features and builds a separate control loop that feeds reference data to the TI loop. TI instaspin-motion is an off the shelf active disturbance rejection controller that is used to develop position, current and/or speed controllers at the motor level. In current controller applications, it takes an input reference current and current feedback from shunts within the motor shield to develop a closed loop control for motor performance. The output of the controller provides a reference current to its field oriented control module. Based on the current reference, the field oriented control module produces a pulse width modulation (PWM) pattern that is then sent to the motor. Figure 6.1 shows a block diagram of the Instaspin motion control scheme. This control loop was chosen for its ease of tuning as only one parameter, bandwidth, must be altered to accurately tune system performance.

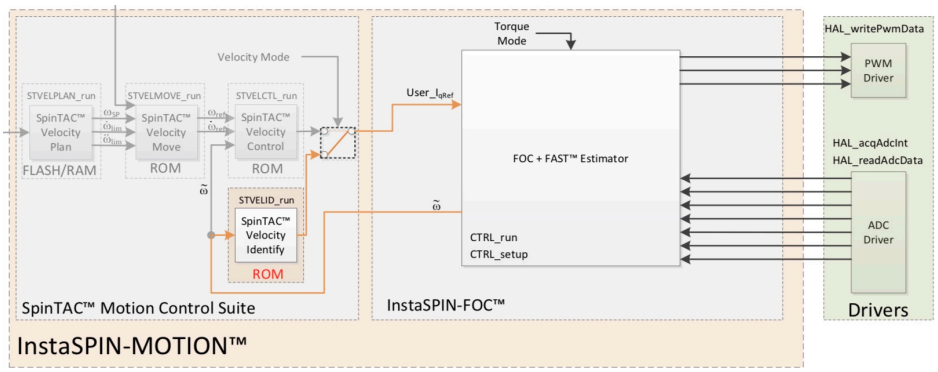

Figure 6.1: TI Instaspin motion Control block diagram

In addition to the Instaspin motion used for motor level control, a proportional-Integral-derivative (PID) controller will be designed to monitor exoskeleton output and determine correct current reference to be fed to the motor control loop. This control loop takes torque reference and feedback from load cell and determines correct response based on torque error. Once the appropriate response is determined it is sent to the motor control loop, resulting in motor motion and ultimately actuation. The actuation force in the cable is measured by the load cell, converted to knee torque based on known structure geometry and sent back to the controller, creating a closed loop. Figure 6.2 shows the entire control scheme structure.

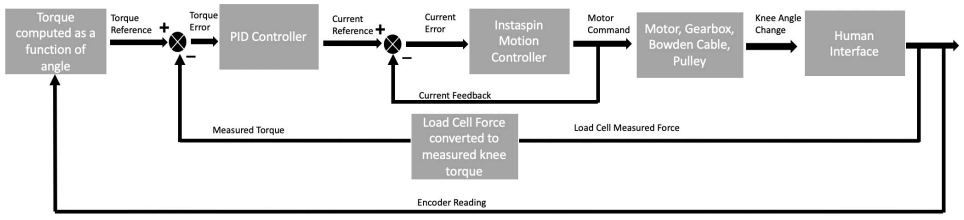

Figure 6.2: Block diagram of a closed loop feedback system that uses load cell reading to better regulate exoskeleton performance

It will also be beneficial to incorporate a high-level controller that monitors and controls human-exoskeleton interaction, allowing for better mechanism control throughout motion profiles. For a high-level controller, I suggest the implementation of a impedance controller

that incorporates readings from the load cell to develop a force control in addition to position control. Typical impedance controllers are an extension of position control and it does not only control position and force but also the relation and interaction between wearer and exoskeleton [52]. The impedance model receives position error of the joint and outputs force reference for the force/torque controller. The force/torque controller will then output a desired exoskeleton force on the wearer. Figure 6.3 presents an example of an impedance controller architecture [18].

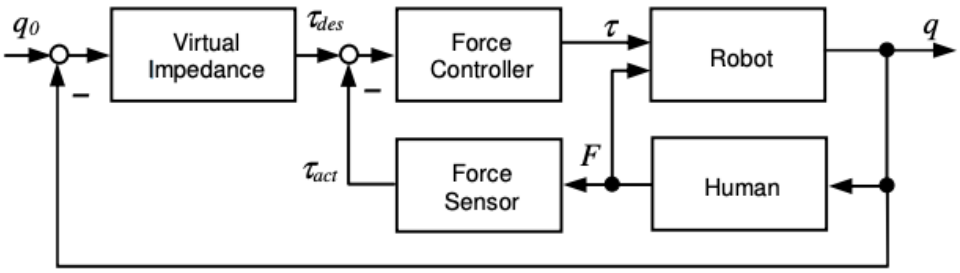

Figure 6.3: Example impedance controller structure used to make a rehabilitation robot compliant [18]

It is also possible to implement an admittance controller which receives forces and outputs positions compared to the impedance which receives position and outputs force. The force error measured will be inputted into the admittance controller and then a reference position will be submitted to the position controller to determine a desired joint angle the exoskeleton aims to reach. Both of these high-level controllers offer more control over human-exoskeleton interaction and allow a variable deviation from a given leg trajectory resulting in more effective operation and an increased level of assistance [18].

6.1.3 Assistance As Needed

The exoskeleton described in this thesis focuses on augmentation of physical capabilities, meaning that it intends to help relatively healthy individuals perform tasks that they struggle

with. This suggest that there is no need to perform the whole task or to provide continuous assistance thus the strategy that should be implemented is AAN. As briefly mentioned in chapter 3, AAN is a type of strategy that takes the wearer's ability and task requirements into account. It is best used to prevent the wearer from becoming over-reliant on assistive devices, as it results in muscle atrophy and neuromotor degradation [46]. AAN will also work to prevent muscle strain and alteration of motion patterns [46]. Adopting this strategy would be a departure from the traditional inverse dynamic method that is currently applied to generate continuous assistance and will often overestimate the amount of assistance needed at various points within movement. AAN will encourage active participation of the wearer.

As part of future work for this exoskeleton, several steps must be taken to implement AAN. First, a method of measuring user muscle capability must be established such as EMG or isometric force testing. Second, determination of the capability gap based on initial muscle performance measurements. Finally, development of a control strategy that accepts the torque requirements of a specific task as input and outputs assistance when the required torque reaches beyond the wearer's measured capabilities.

6.1.4 User intention and Motion Phase recognition

One vital aspect to building a highly effective exoskeleton is the ability to correctly read the wearer's intended movement and/or intended task in real time. This is important because the control system used to predict the wearer's forward trajectory and the correct actuator input can vary greatly among different tasks. As future work of this exoskeleton, it is hoped that a system of user intention detection is developed through the use of either EMG signals that detect possible muscle force generation before human movement or measurements of joint angle, torque, velocities and forces obtained from sensors. Next, take the acquired data

from sensors, create a labeled dataset and input it into a learning algorithm for machine learning. This process will help develop a way in which the exoskeleton becomes predictive of the wearer's intentions. Examples of a few techniques used for movement prediction are presented in Liu (2016), Abhayasinghe (2014) and Chong (2016) [53, 54, 55].

Bibliography

[1] J. Williamson and R. Williams, "Beginning Farmers and Age Distribution of Farmers," 2017.

[2] P. Komdeur, F. E. Pollo, and R. W. Jackson, "Dynamic knee motion in anterior cruciate impairment: a report and case study.," *Proceedings (Baylor University. Medical Center)*, vol. 15, no. 3, pp. 257–9, 2002.

[3] M. Roebroeck, G. Lankhorst, C. Doorenbosch, J. Harlaar, and R. Jacobs, "Biomechanics and muscular activity during sit-to-stand transfer," *Clinical Biomechanics*, vol. 9, no. 4, pp. 235–244, 1994.

[4] M. Schenkman, P. Rlley, R. W. Mann, R. Berger, and W. A. Hodge, "Whole-Body Movements During Rising to Standing from Sitting," *Physical Therapy*, vol. 70, no. 10, pp. 638–651, 1990.

[5] R. Riener, M. Rabuffetti, and C. Frigo, "Stair ascent and descent at different inclinations," *Gait and Posture*, vol. 15, no. 1, p. 32, 2002.

[6] A. N. Lay, C. J. Hass, and R. J. Gregor, "The effects of sloped surfaces on locomotion: A kinematic and kinetic analysis," *Journal of Biomechanics*, vol. 39, no. 9, pp. 1621–1628, 2006.

[7] K. Shamaei, M. Cenciarini, A. A. Adams, K. N. Gregorczyk, J. M. Schiffman, and A. M. Dollar, "Design and evaluation of a quasi-passive knee exoskeleton for investigation of motor adaptation in lower extremity joints," *IEEE Transactions on Biomedical Engineering*, vol. 61, no. 6, pp. 1809–1821, 2014.

[8] K. A. Witte, A. M. Fatschel, and S. H. Collins, "Design of a lightweight, tethered, torque-controlled knee exoskeleton.," *IEEE ... International Conference on Rehabilitation Robotics : [proceedings]*, vol. 2017, pp. 1646–1653, 2017.

[9] A. T. Asbeck, K. Schmidt, I. Galiana, D. Wagner, and C. J. Walsh, "Multi-joint Soft Exosuit for Gait Assistance."

[10] B. Celebi, M. Yalcin, and V. Patoglu, "A SSIST O N -K NEE : A Self-Aligning Knee Exoskeleton," *2013 IEEE/RSJ International Conference on Intelligent Robots and Systems*, pp. 996–1002, 2013.

[11] M. K. Shepherd and E. J. Rouse, "Design and Validation of a Torque-Controllable Knee Exoskeleton for Sit-to-Stand Assistance," *IEEE/ASME Transactions on Mechatronics*, vol. 22, no. 4, pp. 1695–1704, 2017.

[12] K. Junius, B. Brackx, V. Grosu, H. Cuypers, J. Geeroms, M. Moltedo, B. Vanderborght, and D. Lefeber, "Mechatronic Design of a Sit-to-Stance Exoskeleton," *International Conference on Biomedical Robotics and Biomechatronics*, pp. 945–950, 2014.

[13] K. Schmidt, J. E. Duarte, M. Grimmer, A. Sancho-Puchades, H. Wei, C. S. Easthope, and R. Riener, "The myosuit: Bi-articular anti-gravity exosuit that reduces hip extensor activity in sitting transfers," *Frontiers in Neurorobotics*, vol. 11, no. OCT, pp. 1–16, 2017.

[14] R. J. Farris, H. A. Quintero, and M. Goldfarb, "Performance evaluation of a lower limb exoskeleton for stair ascent and descent with Paraplegia," *Proceedings of the Annual International Conference of the IEEE Engineering in Medicine and Biology Society, EMBS*, pp. 1908–1911, 2012.

[15] M. Chandrapal, X. Chen, and W. Wang, "Preliminary evaluation of a lower-limb exoskeleton - Stair climbing," *2013 IEEE/ASME International Conference on Advanced Intelligent Mechatronics: Mechatronics for Human Wellbeing, AIM 2013*, pp. 1458–1463, 2013.

[16] N. Reeves, A. Mohagheghi, C. Maganaris, M. Spanjaard, and V. Baltzopoulos, "Older adults employ alternative strategies to operate within their maximum capabilities when ascending stairs," *Journal of Electromyography and Kinesiology*, vol. 19, no. 2, pp. e57–e68, 2009.

[17] N. D. Reeves, M. Spanjaard, A. A. Mohagheghi, V. Baltzopoulos, and C. N. Maganaris, "The demands of stair descent relative to maximum capacities in elderly and young adults," *Journal of Electromyography and Kinesiology*, vol. 18, no. 2, pp. 218–227, 2008.

[18] R. Riener, M. Frey, M. Bernhardt, T. Nef, and G. Colombo, "Human-centered rehabilitation robotics," *Proceedings of the 2005 IEEE 9th International Conference on Rehabilitation Robotics*, vol. 2005, pp. 319–322, 2005.

[19] W. Van Dijk, H. Van Der Kooij, and E. Hekman, "A passive exoskeleton with artificial tendons: Design and experimental evaluation," *IEEE International Conference on Rehabilitation Robotics*, 2011.

[20] Y. Hasegawa, T. Hoshino, and A. Tsukahara, "Wearable assistive device for physical load reduction of caregiver - Adaptive to caregiver's motion during transferring support," *World Automation Congress Proceedings*, vol. 2016-Octob, pp. 1–6, 2016.

[21] M. de Looze, T. Bosch, F. Krause, K. Stadler, and L. O'Sullivan, "Exoskeletons for Industrial Application and their potential effects on physical work load.pdf," 2016.

[22] R. Grisso, J. Perumpral, S. C. Mariger, D. E. Suttle, K. Funkenbush, and K. Ballin, "Arthritis and Farming," *Virginia Cooperative Extension*, 2009.

[23] J. M. Crawford, G. L. Wilkins, G. L. Mitchell, M. L. Moeschberger, T. L. Bean, and L. A. Jones, "A cross-sectional case control study of work-related injuries among Ohio farmers," *American Journal of Industrial Medicine*, vol. 34, no. 6, pp. 588–599, 1998.

[24] S.-A. Hwang, M. I. Gomez, A. D. Stark, T. Lowery St. John, J. J. May, and E. M. Hallman, "Severe farm injuries among New York farmers," *American Journal of Industrial Medicine*, vol. 40, no. 1, pp. 32–41, 2001.

[25] S. R. Browning, H. Truszczynska, D. Reed, and R. H. Mcknight, "Farmers : The Farm Family Health and Hazard Surveillance Study," *American Journal of Industrial Medicine*, vol. 353, pp. 341–353, 1998.

[26] A. B. Schultz, N. B. Alexander, and J. A. Ashton-Miller, "Biomechanical analyses of rising from a chair," *Journal of Biomechanics*, vol. 25, no. 12, pp. 1383–1391, 1992.

[27] R. Bogue, "Robotic exoskeletons: A review of recent progress," *Industrial Robot*, vol. 42, no. 1, pp. 5–10, 2015.

[28] N. Aliman, R. Ramli, and S. M. Haris, "Design and development of lower limb exoskeletons: A survey," 2017.

[29] F. Sibella, M. Galli, M. Romei, A. Montesano, and M. Crivellini, "Biomechanical analysis of sit-to-stand movement in normal and obese subjects," *Clinical Biomechanics*, vol. 18, no. 8, pp. 745–750, 2003.

[30] R. C. van Lummel, J. Evers, M. Niessen, P. J. Beek, and J. H. van Dieën, "Older adults with weaker muscle strength stand up from a sitting position with more dynamic trunk use," *Sensors (Switzerland)*, vol. 18, no. 4, pp. 1–12, 2018.

[31] S. Yoshioka, A. Nagano, D. C. Hay, and S. Fukashiro, "Peak hip and knee joint moments during a sit-to-stand movement are invariant to the change of seat height within the range of low to normal seat height," *BioMedical Engineering Online*, vol. 13, no. 1, pp. 1–13, 2014.

[32] W. G. Janssen, H. B. Bussmann, and H. J. Stam, "Determinants of the Sit-to-Stand Movement : A Review," *Physical Therapy*, vol. 82, no. 9, 2002.

[33] M. M. Gross, P. J. Stevenson, S. L. Charette, G. Pyka, and R. Marcus, "Effect of muscle strength and movement speed on the biomechanics of rising from a chair in healthy elderly and young women," *Gait and Posture*, vol. 8, no. 3, pp. 175–185, 1998.

[34] D. L. Kowalk, J. A. Duncan, and C. L. Vaughan, "Abduction adduction moments at the knee during stair ascent and descent," *Journal of Biomechanics*, vol. 29, no. 3, pp. 383–388, 1996.

[35] J. M. Aldridge, J. T. Sturdy, and J. M. Wilken, "Stair ascent kinematics and kinetics with a powered lower leg system following transtibial amputation," *Gait and Posture*, vol. 36, no. 2, pp. 291–295, 2012.

[36] M. S. Redfern and J. DiPasquale, "Biomechanics of descending ramps," *Gait and Posture*, vol. 6, no. 2, pp. 119–125, 1997.

[37] J. R. Franz and R. Kram, "Advanced age and the mechanics of uphill walking: A joint-level, inverse dynamic analysis," *Gait and Posture*, vol. 39, no. 1, pp. 135–140, 2014.

[38] A. B. Zoss, H. Kazerooni, and A. Chu, "Biomechanical Design of the Berkeley Lower Limb Exoskeleton (BLEEX)," *IEEE/ASME Transactions on Mechatronics*, vol. 11, no. 2, pp. 128–138, 2006.

[39] Y. L. Park, J. Santos, K. G. Galloway, E. C. Goldfield, and R. J. Wood, "A soft wearable robotic device for active knee motions using flat pneumatic artificial muscles," *Proceedings - IEEE International Conference on Robotics and Automation*, pp. 4805–4810, 2014.

[40] H. Kawamoto, Suwoong Lee, S. Kanbe, and Y. Sankai, "Power assist method for HAL-3 using EMG-based feedback controller," pp. 1648–1653, 2004.

[41] A. Schiele, P. Letier, R. van der Linde, and F. van der Helm, "Bowden Cable Actuator for Force-Feedback Exoskeletons," *International Conference on Intelligent Robots and Systems*, pp. 3599–3604, 2006.

[42] P. T. Cheng, S. H. Wu, M. Y. Liaw, A. M. Wong, and F. T. Tang, "Symmetrical body-weight distribution training in stroke patients and its effect on fall prevention," *Archives of Physical Medicine and Rehabilitation*, vol. 82, no. 12, pp. 1650–1654, 2001.

[43] K. E. Roach and T. P. Miles, "Normal hip and knee active range of motion: the relationship to age.," *Physical therapy*, vol. 71, no. 9, pp. 656–65, 1991.

[44] S. C. Walpole, G. Stevens, I. Roberts, J. Cleland, D. Prieto-Merino, and P. Edwards, "The weight of nations: an estimation of adult human biomass," *BMC Public Health*, vol. 12, no. 1, 2012.

[45] K. Keller and M. Engelhardt, "Strength and muscle mass loss with aging process. Age and strength loss.," *Muscles, ligaments and tendons journal*, vol. 3, no. 4, pp. 346–50, 2013.

[46] M. Afschrift, F. De Groote, J. De Schutter, and I. Jonkers, "The effect of muscle weakness on the capability gap during gross motor function: A simulation study support-

ing design criteria for exoskeletons of the lower limb," *BioMedical Engineering Online*, vol. 13, no. 1, pp. 1–15, 2014.

[47] R. C. Browning, J. R. Modica, R. Kram, and A. Goswami, "The effects of adding mass to the legs on the energetics and biomechanics of walking," *Medicine and Science in Sports and Exercise*, vol. 39, no. 3, pp. 515–525, 2007.

[48] V. A. D. CAI, B. BRU, P. BIDAUD, V. HAYWARD, V. PASQUI, and F. GOSSELIN, "Experimental Evaluation of a Goniometer for the Identification of Anatomical Joint Motions," no. August, pp. 1255–1262, 2011.

[49] M. Kadaba, H. Ramakrishnan, and M. Wooten, "Measurement of Lower Extremity Kinematics During Level Walking," *Journal of Orthopaedic Research*, no. 8, pp. 383–392, 1990.

[50] M. A. Lafortune, P. R. Cavanagh, H. J. Sommer, and A. Kalenak, "Three-dimensional kinematics of the human knee during walking," *Journal of Biomechanics*, 1992.

[51] H. Kazerooni, "Instrumented harmonic Drives for Robotic COmpliant Maneuvers," in *International Conference on Robotics and Automation*, pp. 2274–2279, 1991.

[52] K. Anam and A. A. Al-Jumaily, "Active exoskeleton control systems: State of the art," in *Procedia Engineering*, 2012.

[53] D. X. Liu, X. Wu, W. Du, C. Wang, and T. Xu, "Gait phase recognition for lower-limb exoskeleton with only joint angular sensors," *Sensors (Switzerland)*, vol. 16, no. 10, pp. 1–21, 2016.

[54] N. Abhayasinghe and I. Murray, "Human Gait Phase Recognition Based on Thigh Movement Computed using IMUs," *2014 IEEE Ninth International Conference on In-*

telligent Sensors, Sensor Networks and Information Processing (ISSNIP), no. April, pp. 1–4, 2014.

[55] E. Chong and F. C. Park, "Movement prediction for a lower limb exoskeleton using a conditional restricted Boltzmann machine," 2016.